

Life-history and deleterious mutation rate coevolution

Piret Avila* and Laurent Lehmann

Department of Ecology and Evolution, University of Lausanne
Biophore, 1015 Lausanne, Switzerland

*Corresponding author: piret.avila@gmail.com.

Author contributions: All authors gave final approval for publication and each agreed to be held accountable for all the parts of the work performed therein.

Acknowledgements: -

Data Accessibility Statement: The proofs of the analysis written in Mathematica and the code for individual-based simulations are available in the S.I. as a Mathematica notebook.

Abstract

The cost of germline maintenance gives rise to a trade-off between lowering the deleterious mutation rate and investing into life-history functions. Life-history and the mutation rate therefore coevolve, but this joint evolutionary process is not well understood. Here, we develop a mathematical model to analyse the long-term evolution of individual resource allocation traits affecting life-history and the deleterious mutation rate. We show that the invasion fitness of alleles controlling allocation to life-history functions and mutation rate reduction can be approximated by the basic reproductive number of the least-loaded class, which is the expected lifetime production of offspring without deleterious mutations born to individuals with no deleterious mutations. Second, we analyse two specific biological scenarios: (i) coevolution between reproductive effort and germline maintenance and (ii) coevolution between age at maturity and germline maintenance. This provides two broad biological predictions. First, resource allocation to germline maintenance, at the expense of allocation to survival and reproduction, tends to increase as external causes of mutation rate increase (e.g. environmental stress, oxygen levels) and to tilt allocation towards reproduction instead of survival. Second, when such external causes increase, life-histories tend to be faster with individuals having shorter life spans and smaller body sizes at maturity.

Keywords: life-history evolution, mutation accumulation, adaptive dynamics, cost of fidelity, mutation rate evolution

1 Introduction

Maintaining and accurately transmitting genetically encoded information is central for every living organism. Mutations induce errors in the processing of genetic information and their effects on fitness are generally (mildly) deleterious (Eyre-Walker and Keightley, 2007). Therefore, it is likely that selection primarily favours a reduction of the mutation rate of organisms (Sniegowski et al., 2000). Yet, investing resources into germline maintenance is physiologically costly (Kirkwood, 1986; Maklakov and Immler, 2016; Monaghan and Metcalfe, 2019; Chen et al., 2020). Therefore, the balance between selection against deleterious mutations driving for lower mutation rates and selection for reduced physiological cost increasing mutation rates are expected to lead to a positive evolutionary equilibrium rate of mutation. This argument has been formalised in a number of classical population genetic models assuming semelparous reproduction (e.g. Kimura, 1967; Kondrashov, 1995; Dawson, 1998, 1999; Johnson, 1999; André and Godelle, 2006; Gervais and Roze, 2017) as well as age-structured populations (Lesaffre, 2021) to show that evolution indeed favours a positive evolutionary stable mutation rate. These studies emphasise the role of physiological cost of germline fidelity in explaining the patterns of mutation rates, but do not connect the cost of germline fidelity explicitly to life-history evolution, which depends on underlying physiological trade-offs.

Indeed, a central premise made in life-history theory is that life-history trade-offs are mediated through allocation of resources to different life-history functions, such as growth, reproduction, and maintenance of soma, or information gathering and processing (Stearns, 1992; Roff, 2008). Since germline maintenance takes a toll on available resources, mutation rate evolution and life-history evolution are tied together through a resource allocation trade-off. This implies that the rate of deleterious mutations should co-evolve with life-history and affects various life-history traits, such as reproductive effort, age-at-maturity, adult body size, and expected lifespan. Yet the bulk of models about the evolution of mutation rates, which often go under the heading of modifier models, consider physiologically neutral mutation rate (e.g. Leigh, 1970; Gillespie, 1981; Holsinger and Feldman, 1983; Liberman and Feldman, 1986; Gerrish et al., 2007; Altenberg et al., 2017; Baumdicker et al., 2020). And while the effect of fixed mutation rate on life-history trade-offs have been studied before (e.g. Charlesworth, 1990; Dańko et al., 2012), these models suggest that a relatively high level of mutation rates is needed for mutation accumulation to alter life-history trade-offs. This led to the conclusion that mutation accumulation is a minor force in shaping life-history traits (Dańko et al., 2012). But these studies view mutation rates as fixed traits acting only as a hindrance for adaptive life-history evolution. Hence, no study has yet investigated the joint adaptive coevolution of both deleterious mutation rates and general life-histories in age-structured populations.

The aim of this paper is to start to fill this gap by formally extending evolutionary invasion analysis—“ESS” theory—(e.g., Maynard Smith, 1982; Eshel and Feldman, 1984; Metz et al., 1992; Charlesworth, 1994), which has been sometimes implicitly yet routinely applied to life-history evolution (e.g., León, 1976; Michod, 1979; Schaffer, 1982; Iwasa and Roughgarden, 1984; Stearns, 1992; Perrin, 1992; Perrin

and Sibly, 1993; Cichon and Kozłowski, 2000; Iwasa, 2000; Day and Taylor, 2000), to the case where life-history trait(s) evolving by selection also control the rate of deleterious mutations. This covers the situation where life-history resource allocation schedules evolve on a background where deleterious mutation accumulation can occur. Our formalisation thus aims at integrating both the standard theories of life-history evolution and deleterious mutation accumulation for direct selection on the mutation rate.

The rest of this paper is organised into two parts. First, we characterise the invasion process of a mutant life-history trait affecting the load of deleterious mutations accumulation in an age-structured population. We show that ascertaining the joint evolutionary stability of life-history schedules and mutation rates of deleterious mutations is usually complicated, but under certain biologically feasible conditions; in particular, when the zero mutation class (least-loaded class) dominates the population in frequency, evolutionary stability can be ascertained from the basic reproductive number of the least-loaded class alone (expected lifetime production of offspring with no mutations born to individuals with no mutations). Second, we analyse and solve two concrete biological scenarios: (i) coevolution between reproductive effort and germline maintenance, where individuals face a trade-off between allocating resources to survival, reproduction and germline maintenance and (ii) coevolution between age-at-maturity and germline maintenance, where individuals face a trade-off between allocating resources to growth, reproduction and germline maintenance. These scenarios allow us to illustrate how our model can be applied to analyse questions in life-history and mutation rate evolution and provide predictions about how life-history and the mutation rate coevolves. It also allows us to verify that the analysis based on using the basic reproductive number of the least-loaded class as an invasion fitness proxy matches with results from individual-based stochastic simulations.

2 Model

2.1 Main biological assumptions

We consider a panmictic population of haploid individuals reproducing asexually. The population size is assumed to be large and regulated by density-dependent competition. Individuals in the population are structured into age classes and each individual undergoes birth, possibly development, reproduction, and death. An individual of age a , which is either a discrete or continuous number, is characterised to be of type $\theta(a) = (\mathbf{u}(a), n_m(a))$, which consists of two genetically determined components (see Table 1 for a list of symbols and more formalities). The first component, $\mathbf{u}(a)$, is the individual's life-history trait expressed at age a ; namely, a resource allocation decision at age a to different life-history functions (e.g. growth, reproduction, or somatic maintenance, see e.g. Stearns, 1992; Perrin, 1992; Perrin and Sibly, 1993; Day and Taylor, 2000). We denote by $\mathbf{u} = \{\mathbf{u}(a)\}_{a \in \mathcal{T}}$ the whole life-history schedule or a path over all possible age classes \mathcal{T} an individual can be in (formally, $\mathbf{u} \in \mathcal{U}[\mathcal{T}]$, where $\mathcal{U}[\mathcal{T}]$ is the set of all admissible life-history schedules). The second component, $n_m(a)$, represents the number of deleterious germline mutations an individual at age a carries. Hence, $n_m(a)$ can be thought of as the load

of deleterious mutations as considered in classical population genetic models of mutation accumulation (e.g., Kimura and Maruyama, 1966; Haigh, 1978; Dawson, 1999; Bürger, 2000), but here extended to an age-structured model (see also Steinsaltz et al., 2005 for aged-structured mutation accumulation model). As such, $n_m = \{n_m(a)\}_{a \in \mathcal{J}}$ represents the profile of deleterious mutations across lifespan.

We envision that the genotype determining the type $\theta = (\mathbf{u}, n_m)$ of an individual consists of two separate positions (or loci) that are necessarily linked under asexual reproduction, one locus determining \mathbf{u} and the other n_m (see Fig. 1). The mutation rate at the life-history trait \mathbf{u} locus is assumed to be fixed and is thus exogenously given. However, this trait is assumed to control allocation to germline maintenance and other life-history functions, and thus to control the mutation rate at the locus where the n_m deleterious mutations accumulate whose number are thus endogenously determined (Fig. 1).

We assume that the effective number of births $b(a)$ and the death $d(a)$ of an individual of age a can depend on both the number of deleterious mutations $n_m(a)$ at age a and the life-history schedule \mathbf{u} . The life history schedule \mathbf{u} thus not only affects the vital rates, as usually assumed in life-history theory, but also the rate of deleterious mutation accumulation (see also Fig. 1). The vital rates may further depend on properties of the population, such as age class densities and allele frequencies, but we leave this dependence implicit for now. We note that when measured on an exponential scale, the death and mutation rates define a survival probability $\exp(-d(a))$ and an immutability probability $\exp(-\mu(a))$ (probability that no mutations occur in an individual of age a). Note that for a discrete time process the birth function $b(a)$ gives the expected number of offspring produced by an individual of age a , while for a continuous time process $b(a)$ is defined as the rate at which an individual produces a single offspring. Finally, we make the following *mutational monotonicity assumption*, which will be central in our analysis.

1. Mutations at the locus determining n_m can only be deleterious or neutral. The effective birth rate $b_i(a)$, survival probability $\exp(-d_i(a))$, and immutability probability $\exp(-\mu_i(a))$ of an individual at age a with $n_m(a) = i$ mutations are non-increasing functions of the number of mutations. Formally, $b_i(a) \geq b_{i+1}(a)$, $d_i(a) \geq d_{i+1}(a)$, and $\mu_i(a) \geq \mu_{i+1}(a)$.
2. Mutations can only accumulate within an individual. There are no back mutations and an individual with i mutations can only mutate towards having $i + 1$ mutations.

We are concerned in this paper with formalising selection at the life-history locus. Namely, the objective of our analysis is to develop a tractable evolutionary invasion analysis to evaluate candidate evolutionary stable life-history trait $u^* \in \mathcal{U}[\mathcal{J}]$ that will be favoured by long-term evolution.

2.2 Invasion analysis for life-history with mutation accumulation

2.2.1 Invasion analysis

Evolutionary invasion analysis (e.g., Eshel and Feldman, 1984; Parker and Maynard Smith, 1990; Metz et al., 1992; Charlesworth, 1994; Ferrière and Gatto, 1995; Eshel, 1996; Otto and Day, 2007; Mullon et al., 2016) could be applied straightforwardly to our model in the absence of deleterious mutations as

follows. Mutations at the life-history trait are postulated to be very rare so that one can focus on the invasion fitness $\rho(\mathbf{u}, \mathbf{v})$ of a mutant trait \mathbf{u} introduced at low frequency in a population monomorphic for some resident life-history trait \mathbf{v} that has reached its equilibrium. The invasion fitness is the per capita number of mutant copies produced per unit time by the mutant lineage descending from the initial mutation, when the mutant reproductive process has reached a stationary state distribution (over ages and the number of deleterious mutations) in a resident population and the mutant remains overall rare (i.e. geometric growth ratio of the mutant). Traits that are resistant to invasion define candidate endpoints of evolution and are found by maximising the invasion fitness of the mutant holding the resident at the uninvadable population state. In others words, an uninvadable trait \mathbf{u}^* is a best response to itself; namely

$$\mathbf{u}^* \in \arg \max_{\mathbf{u} \in \mathcal{U}[\mathcal{T}]} \rho(\mathbf{u}, \mathbf{u}^*), \quad (1)$$

so that in the resident population state \mathbf{u}^* , no mutant trait deviation can increase invasion fitness.

To be a meaningful endpoint of evolution, an uninvadable trait needs to be an attractor of the evolutionary dynamics and thus be convergence stable (Eshel and Motro, 1988; Geritz et al., 1998; Leimar, 2009). When mutant and resident traits are sufficiently close to each other so that selection is weak, the gradient of invasion fitness—the selection gradient—is sufficient to determine whether a given mutant can, not only invade the resident population, but also become fixed in it (the so-called “invasion implies substitution” principle applying to the present and more complex demographic scenarios, Rousset, 2004; Priklopil and Lehmann, 2021). As a result, invasion fitness alone under weak phenotypic deviations allows to determine whether gradual evolution under the constant influx of mutations will drive a population towards the uninvadable trait. An evolutionary invasion analysis thus generally consists in both using invasion fitness to (i) characterise uninvadable traits (ii) and to determine whether these are attractors of the evolutionary dynamics, thus allowing to make definite statements about co-evolutionary dynamics. A useful summary of (co)-evolutionary adaptive dynamics concepts can be found in Geritz et al. (1998) and individual-based stochastic simulations have repeatedly validated the conclusions of this approach in genetic explicit contexts (e.g., Mullan et al., 2018; Mullan and Lehmann, 2019, see also Otto and Day, 2007; Dercole and Rinaldi, 2008 for textbook discussions).

This procedure to characterise stable and attainable life histories has been in use more or less explicitly in standard life-history theory for decades (e.g., León, 1976; Michod, 1979; Schaffer, 1982; Iwasa and Roughgarden, 1984; Perrin, 1992; Perrin and Sibly, 1993; Charlesworth, 1994; Day and Taylor, 2000; Cichon and Kozłowski, 2000; Iwasa, 2000; Irie and Iwasa, 2005; Metz et al., 2016; Avila et al., 2019). We now push forward this approach into the realm where life-history evolution interacts with mutation accumulation and thus relax the standard life-history theory assumption that the rate of deleterious mutations is zero. For this case, we still assume that mutations at the life-history locus are rare enough so that whenever a mutant trait \mathbf{u} arises, it does so in a resident population monomorphic for some resident life-history trait \mathbf{v} . But owing to the occurrence of deleterious mutations, the resident population

will be polymorphic for the number of deleterious mutations, and this polymorphism will depend on \mathbf{v} . The resident population is then assumed to have reached a mutation-selection equilibrium for deleterious mutations and the resident trait \mathbf{v} thus determines a resident probability distribution $\mathbf{p}(\mathbf{v})$ over the different number of deleterious mutations carried by individuals across the different age-classes. This assumption is nothing else than the usual assumption of the internal stability of the resident population used in invasion analysis (see e.g. Altenberg et al., 2017; Eshel and Feldman, 1984; Metz et al., 1992). Here, it entails that the resident population has reached an equilibrium for both demographic and genetic processes.

In the absence of age-classes, $\mathbf{p}(\mathbf{v})$ is the equilibrium probability distribution for the number of deleterious mutations in standard selection-mutation balance models (see Bürger, 2000 for a general treatment and where the sample space of $\mathbf{p}(\mathbf{v})$ reduces to \mathbb{N}). For instance, when the number of novel (deleterious) mutations follows a Poisson distribution with mean rate μ and each additional mutation decreases baseline fecundity by a constant multiplicative factor σ in a semelparous population, then $\mathbf{p}(\mathbf{v})$ is Poisson distributed with mean μ/σ (Haigh, 1978, Bürger, 2000, p. 300). This holds in an age-structured population across age-classes under certain but limited number of conditions (Steinsaltz et al., 2005). More generally, $\mathbf{p}(\mathbf{v})$ will depend on the details of the model.

2.2.2 Invasion process with mutation accumulation

Since the mutant trait \mathbf{u} can arise in individuals carrying different numbers of deleterious mutations, the invasion process of \mathbf{u} is contingent on the genetic background in which it arises, and we refer to the initial carrier of the \mathbf{u} trait as the progenitor (or ancestor) of \mathbf{u} . The invasion fitness of \mathbf{u} is then determined by the size of the lineage of the progenitor, which consists of all of its descendants carrying \mathbf{u} far into the future. Namely, the immediate descendants of the progenitor including the surviving self, the immediate descendants of the immediate descendants, etc., covering the whole family history tree *ad infinitum*. Crucially, descendants may accumulate deleterious mutations during the process of initial growth or extinction of the mutant lineage when this lineage is rare (referred to throughout as the “invasion process”). As such, the invasion process, whether it occurs in continuous or discrete time, can be regarded as a multitype age-dependent branching process (Mode, 1968, 1971) since during growth or extinction, novel genotypes are produced by mutation. To analyse this process, it is useful to organise individuals into *equivalence classes*. The defining feature of an equivalence class is that it is a collection of states of a process among which transitions eventually occur, so the states are said to communicate (Karlin and Taylor, 1975, p. 60). The equivalence class \mathcal{C}_i will stand for all mutant individuals carrying i deleterious mutations and thus consist of individuals of all age classes. This is an equivalence class because through survival and reproduction, an individual of any age with i mutations may eventually transition to become an individual of any other age (in the absence of menopause). This follows from the fact that the process of survival and reproduction in an age-structured population in the absence of mutations (and menopause) is irreducible (Caswell, 2000). Indeed, starting in any age-class, eventually

every age-class can be reached. Owing to the mutational monotonicity assumption, however, starting in a given class, it is possible to enter another class, but not transition back from that class (otherwise the two classes would form a single class). The mutant population process is thus overall reducible and can be regarded as a reducible multitype age-dependent branching process (Nair and Mode, 1971; Mode, 1971). We say that equivalence class \mathcal{C}_{i+1} follows class \mathcal{C}_i since individuals in equivalence class i can only transition to class $i + 1$ by acquiring mutations.

To see why the notion of equivalence class is useful to understand the invasion process, let us focus on a discrete time process with discrete age classes; namely, $\mathcal{T} = \{0, 1, 2, \dots, T\}$ and denote by $n_i(t)$ the expected number of individuals at time t in class \mathcal{C}_i that descend from a single class \mathcal{C}_i newborn ancestor born t time-units ago (i.e. $n_i(0) = 1$). Then, accounting for all the descendants of the progenitor (including the surviving self) entails that $n_i(t)$ satisfies the renewal equation

$$n_i(t) = \tilde{l}_i(t) + \sum_{a=0}^t n_i(t-a) \tilde{b}_i(a) \tilde{l}_i(a), \quad (2)$$

where $\tilde{l}_i(a)$ is the probability that a \mathcal{C}_i class newborn survives to age a and has not acquired any new mutations (we assume that $\tilde{l}_i(a) \rightarrow 0$ as $a \rightarrow \infty$, since death or mutation must eventually occur). The quantity $\tilde{b}_i(a)$ is the expected number of (newborn) offspring without new mutations produced by an individual of age a that carries i deleterious mutations. Hence, the first term on the right-hand-side of eq. (2) accounts for the survival and immutability of the ancestor itself until age t . The second term projects the expected number of individuals without mutations descending from the progenitor at $t - a$ (and for all $a \leq t$) into new lineage members without mutation at t . Together, these two terms thus give the total lineage size of the progenitor and a key feature of eq. (2) is that it depends only on the vital rates and states of individuals of class \mathcal{C}_i . As such, eq. (2) is functionally equivalent to the standard renewal equation of population dynamics in discrete age-structured populations (Charlesworth, 1994, eq. 1.34). It then follows from standard results (e.g., Charlesworth, 1994, p. 25-26) that asymptotically, as $t \rightarrow \infty$, the number $n_i(t)$ grows geometrically as

$$n_i(t) \sim \rho_i^t K_i, \quad (3)$$

where K_i is a constant depending on the process and ρ_i is the unique root satisfying the characteristic (or Euler-Lotka) equation $\sum_{a=0}^T \rho_i^{-a} \tilde{l}_i(a) \tilde{b}_i(a) = 1$.

Since individuals of class i contribute to individuals of class $i + 1$ through mutations (the equivalence class \mathcal{C}_{i+1} follows class \mathcal{C}_i), then $n_i(t)$ does not describe the total expected lineage size of the progenitor. However, owing to the mutational monotonicity assumption, the growth ratio ρ_i is at least as large as ρ_{i+1} , i.e., $\rho_i \geq \rho_{i+1}$ for all i . This implies that when the ancestor is of type i , the expected lineage size is determined by the growth ratio ρ_i , since it dominates that of any other following equivalence class. Hence, asymptotically, the total expected lineage of an \mathcal{C}_i class progenitor has geometric growth ratio ρ_i . It further follows from the theory of multitype age-dependent branching processes that the realised lineage

size of a single progenitor (a random variable) has growth ratio ρ_i if $\rho_i > 1$ and otherwise, if $\rho_i \leq 1$, the lineage goes extinct with probability one (Mode, 1971, Theorem 7.2 p. 245, Corrolary 6.1 p. 280, see also Mode, 1968 for the single type case). Further, $\rho_i \leq 1$ if (and only if) $\tilde{R}_i \leq 1$, where $\tilde{R}_i = \sum_{a=0}^T \tilde{l}_i(a) \tilde{b}_i(a)$ is the expected number of offspring of the progenitor produced throughout its lifespan (i.e. Mode, 1971, Theorem 7.2 p. 245, Corrolary 6.1 p. 280, see also Karlin and Taylor, 1981, p. 424, Caswell, 2000). Hence, ρ_i is an appropriate measure of invasion fitness and \tilde{R}_i is an appropriate proxy of it, for a type i mutant \mathbf{u} arising in an resident \mathbf{v} background (for a discussion of various biological representations of invasion fitness and proxies thereof see Lehmann et al., 2016). The same argument can be made for continuous time processes, in which case $\rho_i = \exp(r_i)$, where r_i is the rate of natural increase of the lineage size of a progenitor of type i , i.e., the Malthusian growth rate (see Appendix A).

2.3 Uninvadability for dominating least loaded class

The key feature of the invasion process in a population with distinct mutational equivalence classes is that the invasion of a mutant depends on the class in which it appears (ρ_i for class i), which in turn depends on the distribution $\mathbf{p}(\mathbf{v})$. This means that there are as many growth rates as equivalence classes, since the invasion process is reducible (see also Altenberg, 2009, p. 1278). Therefore characterising long-term evolution using a single representation of invasion fitness (or proxy thereof) is at first glance unattainable under our modelling assumptions. Yet, as a first-step, it also seems reasonable to consider a situation where the mutation-selection process is such that the least-loaded class \mathcal{C}_0 dominates the population in frequency (i.e. the frequency of the zero-class individuals is close to one). If selection is stronger than mutation, then deleterious alleles will tend to be purged and the mutation-selection balance will be far away from the error threshold of mutation accumulation or meltdown of asexual populations (e.g., Eigen, 1971; Lynch et al., 1993; Szathmary and Maynard Smith, 1997). For instance, in the classical mutation-selection equilibrium model mentioned in section 2.2.1 (Haigh, 1978, Bürger, 2000), the frequency of the zero mutation class is $e^{-\mu/\sigma}$. So when $\mu \ll \sigma$, say for definiteness the selection coefficient is one order of magnitude larger than the mutation rate (e.g. for $\mu = 0.01$ and $\sigma = 0.1$, $\mu/\sigma = 0.1$), then the least loaded class dominates in frequency ($e^{-\mu/\sigma} \approx 0.9$). Under these conditions, the click rate of Muller's ratchet (Muller's ratchet is said to click when the class of individuals with the least amount of deleterious mutations in the population becomes extinct) is small for finite but sufficiently large population sizes. For instance, in a population of size $N = 1000$, the click rate is 8.4×10^{-34} (obtained from $1/\tau$ where $\tau = \sigma \sqrt{2\pi N/\mu} \times \exp\left(N(\sigma - \mu(1 - \log(\frac{\mu}{\sigma})))\right)/(\sigma - \mu)^2$ is the inverse of the click rate, see eq. 23 Metzger and Eule, 2013, where $\sigma = s$ and $\mu = u$). Hence, the click rate of Muller's ratchet can be considered negligible compared to the scale of mutation rates. Thus, whenever the selection coefficient is one order of magnitude larger than the mutation rate, whenever a mutant life-history trait \mathbf{u} appears in a resident \mathbf{v} population, it is likely to arise on a zero mutation background (i.e. in class \mathcal{C}_0 individuals).

Endorsing the assumption that the least-loaded class dominates in frequency then allows to characterise the fate of mutant \mathbf{u} appearing in a resident \mathbf{v} population (recall eq. 1) directly from the growth

ratio

$$\rho(\mathbf{u}, \mathbf{v}) = \rho_0(\mathbf{u}, \mathbf{v}), \quad (4)$$

of the least-loaded class. Further, since $\rho_0(\mathbf{u}, \mathbf{v}) \leq 1 \iff \tilde{R}_0(\mathbf{u}, \mathbf{v}) \leq 1$, where $\tilde{R}_0(\mathbf{u}, \mathbf{v})$ is the basic reproductive number of the least-loaded class, i.e. the expected number of class \mathcal{C}_0 offspring produced by a class individual \mathcal{C}_0 individual over its lifespan, is sufficient to characterise the fate of the mutant. It then follows that an uninvadable strategy \mathbf{u}^* can be characterised in a discrete age-structured population as

$$\mathbf{u}^* \in \arg \max_{\mathbf{u} \in \mathcal{U}[\mathcal{T}]} \tilde{R}_0(\mathbf{u}, \mathbf{u}^*), \quad (5)$$

which entails maximising (in the best response sense) the basic reproductive number of the least-loaded class. Likewise, multi-dimensional convergence stability (Lessard, 1990; Leimar, 2009) can be assessed from $\tilde{R}_0(\mathbf{u}, \mathbf{u}^*)$. And this reproductive number is given explicitly in terms of vital rates by

$$\tilde{R}_0(\mathbf{u}, \mathbf{v}) = \sum_{a=0}^T \tilde{b}_0(a, \mathbf{u}, \mathbf{v}) \tilde{l}_0(a, \mathbf{u}, \mathbf{v}), \quad (6)$$

where

$$\tilde{b}_0(a, \mathbf{u}, \mathbf{v}) = b_0(a, \mathbf{u}, \mathbf{v}) \times \exp(-\mu_f(a, \mathbf{u}, \mathbf{v})) \quad (7)$$

and

$$\tilde{l}_0(a, \mathbf{u}, \mathbf{v}) = l_0(a, \mathbf{u}, \mathbf{v}) \times \exp\left(-\sum_{t=0}^{a-1} \mu_s(t, \mathbf{u}, \mathbf{v})\right) \quad \text{with} \quad l_0(a, \mathbf{u}, \mathbf{v}) = \prod_{t=0}^a s_0(t, \mathbf{u}, \mathbf{v}). \quad (8)$$

Here, $b_0(a, \mathbf{u}, \mathbf{v})$ is the effective fecundity of an individual of age a who has no mutations, $s_0(a, \mathbf{u}, \mathbf{v}) = \exp(-d_0(a, \mathbf{u}, \mathbf{v}))$ is the probability that such an individual survives over the age interval $[a, a + 1]$ (and $d_0(a, \mathbf{u}, \mathbf{v})$ is its death rate), and $l_0(a, \mathbf{u}, \mathbf{v})$ is the probability of survival to age a . In eqs. (7)–(8), we have distinguished between the mutation rate during reproduction $\mu_f(a, \mathbf{u}, \mathbf{v})$, which is the rate of mutations in newborn offspring while the parent giving birth is of age a , and the mutation rate during lifespan $\mu_s(a, \mathbf{u}, \mathbf{v})$, which is the rate of germline mutations in an organism of age a . Note that the vital rates $b_0(a, \mathbf{u}, \mathbf{v})$ and $s_0(a, \mathbf{u}, \mathbf{v})$ depend on the resident population and can thus be possibly affected by density-dependent regulation. When $\mu_f(a, \mathbf{u}, \mathbf{v}) = \mu_s(a, \mathbf{u}, \mathbf{v}) = 0$ for all $a \in \mathcal{T}$, eq. (6) reduces to the standard basic reproductive number for age-structured populations (e.g. Charlesworth, 1994). We emphasise that we allowed for fecundity, survival and mutation rate to be dependent on the whole life history schedule because the evolving traits may affect physiological state variables (e.g. body size). As long as there is a direct correspondence between age and physiological state (see e.g. the discussion in de Roos, 1997), then

the extension of current formalisation to physiologically-structured populations is direct (see also section 3.2 for an example). Furthermore, individuals can also be affected by the (physiological) state variables of other individuals (e.g. size-dependent competition) and hence our formulation implicitly covers these situations and frequency- and density-dependent interactions more generally.

For a continuous time process with a continuous age structure ($\mathcal{T} = [0, T]$), we show in Appendix A that the basic reproductive number of the least-loaded class is

$$\tilde{R}_0(\mathbf{u}, \mathbf{v}) = \int_0^T \tilde{b}_0(a, \mathbf{u}, \mathbf{v}) \tilde{l}_0(a, \mathbf{u}, \mathbf{v}) da, \quad (9)$$

where $\tilde{b}_0(a, \mathbf{u}, \mathbf{v})$ takes the same functional form as in eq. (7) but is now interpreted as the effective birth rate (of offspring with no mutations) at age a , and $\tilde{l}_0(a, \mathbf{u}, \mathbf{v})$ satisfies the differential equation:

$$\frac{d\tilde{l}_0(a, \mathbf{u}, \mathbf{v})}{da} = -[d_0(t, \mathbf{u}, \mathbf{v}) + \mu_s(t, \mathbf{u}, \mathbf{v})] \tilde{l}_0(a, \mathbf{u}, \mathbf{v}) \quad \text{subject to} \quad \tilde{l}_0(0, \mathbf{u}, \mathbf{v}) = 0. \quad (10)$$

We now make four observations on the use of $\tilde{R}_0(\mathbf{u}, \mathbf{v})$ to characterise long-term coevolution for life-history traits and mutation rates. (1) Because $\tilde{R}_0(\mathbf{u}, \mathbf{v})$ depends on the amount of deleterious mutations in the population solely via \mathbf{v} , the distribution $\mathbf{p}(\mathbf{v})$ is needed only under frequency-dependent selection. This makes life-history evolution in the presence of deleterious mutations tractable even if the underlying evolutionary process of mutation is not (see section eq. 3.2 for an example). The characterisation of uninvasibility using $\tilde{R}_0(\mathbf{u}, \mathbf{v})$ (and thus applying eqs. 4–10) generalises the results of Dawson (1998, p. 148) to overlapping generations and an explicit life-history context (and has been used before in the study of direct selection on a mutation modifier in semelparous populations see e.g. Leigh, 1970; Dawson, 1999). (2) Because $\tilde{R}_0(\mathbf{u}, \mathbf{v})$ takes the standard form of the basic reproductive number, the results of optimal control and dynamic game theory can be applied to characterise uninvasibility. This is useful in particular for reaction norm and developmental evolution and formalising different modes of trait expressions (see Avila et al., 2021). (3) While low mutation rates relative to selection are presumed to be able to use $\tilde{R}_0(\mathbf{u}, \mathbf{v})$ as a proxy for invasion fitness, these mutation rates are endogenously determined by the uninvasible strategy. It is thus plausible that the uninvasible mutation rate generally entails low mutation rate. So the assumption of low mutation rate may not appear so drastic and the extent to which this assumption is limiting depends on investigating explicit evolutionary scenarios. (4) If deleterious mutations are such that all the ρ_i 's are proportional to ρ_0 's, which is the case for the standard mutation accumulation models with multiplicative effect of (deleterious) mutations, then using \tilde{R}_0 does not rely on making the assumption of low mutation rates relative to selection, since regardless in which background the mutation appears, it will grow proportionally to ρ_0 , and so if \tilde{R}_0 is maximised (in the best response sense) so will ρ_0 .

This gives good reasons to use $\tilde{R}_0(\mathbf{u}, \mathbf{v})$ as a proxy of invasion fitness and as such, in the rest of this paper we consider two scenarios of life-history and mutation accumulation coevolution that we analyse by using $\tilde{R}_0(\mathbf{u}, \mathbf{v})$. This allows us to illustrate the different concepts, demonstrate the usefulness of focusing

on $\tilde{R}_0(\mathbf{u}, \mathbf{v})$ to get insights about how life-history evolution interacts with mutation accumulation, and check results against individual-based stochastic simulations.

3 Examples of life-history and mutation rate coevolution

3.1 Coevolution of reproductive effort and germline maintenance

3.1.1 Biological scenario

Our first scenario considers the evolution of reproductive effort when resources can be allocated to (germline) maintenance in an iteroparous population. To that end, we assume a population with a large but fixed number N of individuals undergoing the following discrete time life-cycle. (1) Each of the N adult individuals produces a large number of juveniles and either survives or dies independently of other individuals. Juveniles and surviving adults acquire mutations at the deleterious allele locus at the same rate. (2) Density-dependent competition occurs among juveniles for the vacated breeding spots (left by the dead adults) and the population is regulated back to size N .

We postulate that individuals have a static life-history trait consisting of two components $\mathbf{u} = (u_g, u_s)$ ($\mathbf{u} \in \mathcal{U}[\mathcal{T}] = [0, 1]^2$), which determines how a fixed amount of resources available to each individual is allocated between three physiological functions: (i) a proportion $(1 - u_g)(1 - u_s)$ of resources is allocated to reproduction, (ii) a proportion $(1 - u_g)u_s$ of resources is allocated to survival, and (iii) a proportion u_g of resources is allocated to germline maintenance.

We assume that an individual with trait \mathbf{u} and i deleterious mutations has the following fecundity $f_i(\mathbf{u})$, survival probability $s_i(\mathbf{u})$, and mutation rates $\mu_f(\mathbf{u})$, $\mu_s(\mathbf{u})$ (at giving birth and when surviving to the next generation, respectively),

$$\begin{aligned} f_i(\mathbf{u}) &= f_0(\mathbf{u}) \times (1 - \sigma_f)^i \\ s_i(\mathbf{u}) &= s_0(\mathbf{u}) \times (1 - \sigma_s)^i \\ \mu(\mathbf{u}) &= \mu_s(\mathbf{u}) = \mu_f(\mathbf{u}) = \mu_b (1 - u_g)^{\alpha_\mu}, \end{aligned} \tag{11}$$

where σ_f and σ_s are, respectively, the reductions in fecundity and survival from carrying an additional deleterious mutations (that are assumed to act multiplicatively), μ_b is the baseline mutation rate (mutation rate when allocation to germline maintenance is at its minimum, $u_g = 0$), and α_μ is the maintenance scaling factor (a parameter tuning how investing a unit resource into maintenance translates into reducing the mutation rate). We assume that $\alpha_\mu > 1$, such that $\mu(\mathbf{u})$ has decreasing negative slopes in u_g and hence exhibits diminishing returns from investment into germline maintenance.

The quantities $f_0(\mathbf{u})$ and $s_0(\mathbf{u})$ are, respectively the fecundity and survival of the least-loaded class

and they are written as

$$\begin{aligned} f_0(\mathbf{u}) &= f_b \left((1 - u_s)(1 - u_g) \right)^{\alpha_f} \\ s_0(\mathbf{u}) &= s_b \left(u_s(1 - u_g) \right)^{\alpha_s}. \end{aligned} \tag{12}$$

Here, f_b and s_b are, respectively, the baseline fecundity and baseline probability of survival; α_f and α_s are, respectively, the fecundity and survival scaling factors (parameters tuning how a unit resource translates into fecundity and survival). We assume that $\alpha_f, \alpha_s \leq 1$ whereby both survival and fecundity have decreasing positive slopes in net amount of resources allocated to them and thus exhibit diminishing returns. Lower values of α_f and α_s correspond to more strongly diminishing returns of investing resources into reproduction and survival, respectively. In the absence of mutation rate, the model reduces to the standard model of reproductive effort of life-history theory with trade-off between reproduction and survival (Charnov, 1993; Pen, 2000; Case, 2000). Conversely, with no over-lapping generations and no life-history evolution, the model reduces to the classical model of mutation accumulation (Haigh, 1978; Bürger, 2000), and with zero survival and resource allocation evolution, it is equivalent to the asexual model of Dawson (1998). The model thus combines an unexplored trade-off between life-history traits (survival and reproduction) and immutability (germline maintenance).

3.1.2 Basic reproductive number

From the model assumptions, we have that the survival of the least-loaded class (eq. 8) reduces to

$$\tilde{l}_0(a, \mathbf{u}, \mathbf{v}) = s_0(\mathbf{u})^a \exp(-\mu(\mathbf{u})a) \tag{13}$$

and the effective fecundity of the least-loaded class (eq. 7) can be written as

$$\tilde{b}_0(a, \mathbf{u}, \mathbf{v}) = \tilde{b}_0(\mathbf{u}, \mathbf{v}) = \underbrace{(1 - \bar{s}(\mathbf{v})) \frac{f_0(\mathbf{u})}{\bar{f}(\mathbf{v})}}_{b_0(\mathbf{u}, \mathbf{v})} \exp(-\mu(\mathbf{u})), \tag{14}$$

which depends on the mean survival and fecundity in the population, respectively, $\bar{s}(\mathbf{v}) = \sum_{k=0}^{\infty} s_k(\mathbf{v})p_k(\mathbf{v})$ and $\bar{f}(\mathbf{v}) = \sum_{k=0}^{\infty} f_k(\mathbf{v})p_k(\mathbf{v})$. Here, $p_i(\mathbf{v})$ is the probability that an individual randomly sampled from the resident population carries i deleterious mutations (and so $\mathbf{p}(\mathbf{v}) = \{p_i(\mathbf{v})\}_{i \in \mathbb{N}}$ for this model). This can be understood by noting that $(1 - \bar{s}(\mathbf{v}))$ is the fraction of open breeding spots available to a juvenile and the probability that the offspring of a given adult acquires a breeding spot depends on the fecundity of the adult relative to the population average fecundity (as each juvenile is equally likely to acquire a breeding spot).

Since there is no fixed end to lifespan under the above life-cycle assumptions (so $T \rightarrow \infty$) and using

eq. (6) along with eqs. (13)–(14) entails that

$$\tilde{R}_0(\mathbf{u}, \mathbf{v}) = \frac{b_0(\mathbf{u}, \mathbf{v})}{\exp(\mu(\mathbf{u})) - s_0(\mathbf{u})}, \quad (15)$$

(all our mathematical computations can be followed and confirmed via an accompanying Supplementary Information, S.I. consisting of a Mathematica notebook). Since $b_0(\mathbf{u}, \mathbf{v})$ is multiplicatively separable with respect to its arguments then it follows from eq. (15) that the model satisfies the condition of an optimisation principle (e.g., Metz et al., 2008). Namely, $\tilde{R}_0(\mathbf{u}, \mathbf{v}) = F_1(\mathbf{u})F_2(\mathbf{v})$ for the functions $F_1(\mathbf{u}) = f_0(\mathbf{u})/[\exp(\mu(\mathbf{u})) - s_0(\mathbf{u})]$ depending only on the mutant and $F_2(\mathbf{v}) = [1 - \bar{s}(\mathbf{v})]/\bar{f}(\mathbf{v})$ depending only on the resident. It follows that maximising $F_1(\mathbf{u})$ is sufficient to ascertain uninvasibility and uninvasibility implies convergence stability when the evolutionary dynamics follows an optimization principle (Metz et al., 2008). Further, the explicit expressions for $\bar{s}(\mathbf{v})$ and $\bar{f}(\mathbf{v})$, and thus the distribution $\mathbf{p}(\mathbf{v})$ are not needed to carry out the invasion analysis. All this allows to markedly simplify the evolutionary analysis.

We will nevertheless work out the resident distribution $\mathbf{p}(\mathbf{v})$ so as to have a fully worked example that allows for consistency checks and illustrating the concepts. Since we consider a deterministic resident population process, the frequency p_k satisfies at equilibrium the equation

$$p_k(\mathbf{v}) = \sum_{i=0}^k \phi_{k-i}(\mathbf{v})w_i(\mathbf{v})p_i(\mathbf{v}), \quad (16)$$

where $w_i(\mathbf{v}) = s_i(\mathbf{v}) + (1 - \bar{s}(\mathbf{v}))f_i(\mathbf{v})/\bar{f}(\mathbf{v})$ is the individual fitness–survival plus effective fecundity–of an individual with i deleterious mutations, and ϕ_k is the probability that k deleterious mutations are produced upon reproduction. Assuming that the mutation distribution is Poisson with mean $\mu(\mathbf{v})$ and $\sigma_s = \sigma_f = \sigma$, then eq. (16) becomes structurally equivalent to eq. (1) of Haigh (1978) and eq. (5.3) of Bürger (2000, p. 300) (with mean fitness $\bar{w} = 1$ since population size is constant) and as such the equilibrium distribution $\mathbf{p}(\mathbf{v})$ is Poisson with mean $\lambda(\mathbf{v}) = \mu(\mathbf{v})/\sigma$ (see also the section 1.1.1. in SM). This completely characterises the genetic state of the resident population and implies that

$$\bar{s}(\mathbf{v}) = s_0(\mathbf{v})e^{-\mu(\mathbf{v})} \quad \text{and} \quad \bar{f}(\mathbf{v}) = f_0(\mathbf{v})e^{-\mu(\mathbf{v})}. \quad (17)$$

Substituting the explicit expression for the survival and effective fecundities (eq. 17) into eq. (15) shows that in a monomorphic \mathbf{v} population $\tilde{R}_0(\mathbf{v}, \mathbf{v}) = 1$, as required for a consistent model formulation. Eq. (17) generalises the standard mutation-accumulation model of population genetics to overlapping generations with survival probability depending on the number of deleterious mutations (see e.g. eq. 3.3 Kimura and Maruyama, 1966).

3.1.3 Uninvasible and convergence stable strategies

We now carry out the invasion analysis explicitly following the standard approach of working with selection gradients (e.g., Parker and Maynard Smith, 1990; Frank, 2008; Geritz et al., 1998; Rousset, 2004; Mullan

et al., 2016). Using eq. (11), (12), (14), and (17) in eq. (15) and taking the derivative with respect to u_g , we find that the selection gradient on maintenance can be written as

$$\left. \frac{\partial \tilde{R}_0(\mathbf{u}, \mathbf{v})}{\partial u_g} \right|_{\substack{u_g=v_g \\ u_s=v_s}} = \frac{1}{(1-\bar{s}(\mathbf{v}))(1-v_g)} \left(\alpha_\mu \mu(\mathbf{v}) - \left[\alpha_s \bar{s}(\mathbf{v}) + \alpha_f (1-\bar{s}(\mathbf{v})) \right] \right), \quad (18)$$

where the terms in parenthesis display the trade-off between allocating resources into maintenance vs. the two vital rates. The first term in eq. (18) is the marginal benefit of investment into repair, which is a decreasing function of v_g . The second term is the marginal cost of investment into maintenance and this depends on the weighted sum over average survival and open breeding spots. This is a concave function of v_g if $\alpha_s > \alpha_f$, a convex function of v_g if $\alpha_s < \alpha_f$, and independent of v_g if $\alpha_s = \alpha_f = \alpha$. Decreasing α_μ , α_s , and α_f favours allocation of resources to maintenance, since it yields higher returns from investment into germline maintenance (recall that lower values of parameter α_μ means that investing resources into germline maintenance exhibits weaker diminishing returns of investment and lower values of parameters α_f and α_s means that investing resources into fecundity and survival, respectively, exhibits stronger diminishing returns of investment). We find that the selection gradient on survival can be written as

$$\left. \frac{\partial \tilde{R}_0(\mathbf{u}, \mathbf{v})}{\partial u_s} \right|_{\substack{u_g=v_g \\ u_s=v_s}} = \frac{1}{1-\bar{s}(\mathbf{v})} \left(\frac{\alpha_s \bar{s}(\mathbf{v})}{v_s} - \frac{\alpha_f (1-\bar{s}(\mathbf{v}))}{(1-v_s)} \right), \quad (19)$$

where the terms in the parenthesis display the trade-off between allocating resources into survival vs. fecundity. The first term in eq. (19) is the marginal benefit of investments into survival, which is a decreasing function of v_g , while the second term is the marginal benefit of investments into fecundity, and increasing function of v_g . This trade-off is the classical reproductive effort trade-off (e.g., Pen, 2000, eq. 4) with the difference that it is here affected by the mutation rate. In particular, an increase in the baseline mutation rate $\mu_b(v_g)$ favours higher allocation to survival (by increasing $\bar{s}(\mathbf{v})$).

A necessary condition for $(u_g^*, u_s^*) = \mathbf{u}^*$ to be an evolutionary equilibrium is that the selection gradients vanish at this point (for an interior equilibrium, i.e. $0 < u_g^*, u_s^* < 1$), i.e. $\partial \tilde{R}_0(\mathbf{u}, \mathbf{v})/\partial u_s = 0$ and $\partial \tilde{R}_0(\mathbf{u}, \mathbf{v})/\partial u_g = 0$ evaluated at $\mathbf{v} = \mathbf{u} = \mathbf{u}^*$. Without further assumptions on eqs. (18)–(19), we were unable to find such analytical solutions. But setting $\alpha_s = \alpha_f = \alpha$, we find that there is a unique solution

$$u_g^* = \begin{cases} 0 & \text{if } \mu_b \leq \frac{\alpha}{\alpha_\mu} \\ 1 - \left(\frac{\alpha}{\alpha_\mu \mu_b} \right)^{\frac{1}{\alpha_\mu}} & \text{otherwise} \end{cases}, \quad u_s^* = \begin{cases} \left(\frac{\exp(\mu_b)}{s_b} \right)^{\frac{1}{\alpha-1}} & \text{if } \mu_b \leq \frac{\alpha}{\alpha_\mu} \\ \left(\frac{\exp(\frac{\alpha}{\alpha_\mu}) \left(\frac{\alpha}{\alpha_\mu \mu_b} \right)^{-\frac{\alpha}{\alpha_\mu}}}{s_b} \right)^{\frac{1}{\alpha-1}} & \text{otherwise} \end{cases} \quad (20)$$

with corresponding expressions for the mutation rate $\mu(\mathbf{u}^*)$ and mean number of novel (deleterious) mutations $\lambda(\mathbf{u}^*)$ taking the following form

$$\mu(\mathbf{u}^*) = \begin{cases} \mu_b & \text{if } u_g^* = 0 \\ \alpha/\alpha_\mu & \text{if } u_g^* > 0 \end{cases}, \quad \lambda(\mathbf{u}^*) = \begin{cases} \mu_b/\sigma & \text{if } u_g^* = 0 \\ \alpha/(\alpha_\mu \sigma) & \text{if } u_g^* > 0 \end{cases}. \quad (21)$$

Eq. (20) determines the candidate uninvadable and convergence stable trait values. We checked that for biologically realistic parameter values (e.g. for the parameter values in Fig. 2) these trait values are indeed uninvadable and convergence stable using the standard approach (Eshel, 1983; Taylor, 1989; Geritz et al., 1998; Mullan et al., 2016 and see section 1.5.3. in S.I.) and thus are stable attractors of the co-evolutionary dynamics. And while we derived the \mathbf{u}^* assuming $\alpha_f = \alpha_s$ in eq. (20), we numerically checked the robustness of the qualitative behaviour of the results with respect to changes in the values of parameters, such that $\alpha_f \neq \alpha_s$ and we find that overall behaviour of the results remain the same (see section 1.1.4. of S.I.).

Using individual-based stochastic simulations, Fig. (3) demonstrates that the co-evolutionary dynamics indeed converges towards the uninvadable strategy \mathbf{u}^* (eq. 20) predicted by the analytical model. Fig. (2) illustrates the uninvadable life-history strategies $\mathbf{u}^* = (u_g^*, u_s^*)$ (panels a and b), the corresponding mutation rate $\mu(\mathbf{u}^*)$ (panel c) and the mean number of novel mutations $\lambda(\mathbf{u}^*)$ (panel d) as a function of the baseline mutation rate μ_b . We can observe from Fig. (2) that the analytically obtained results (eq. 20–21) correspond very closely to those obtained by carrying out individual-based stochastic simulations of the full process, which implements the life-cycle and assumptions of the present biological scenarios but allows for mutation at the life-history locus (e.g. Fig. 1 and see Appendix B for the description of the simulations and the S.I. for the Mathematica code of the simulations). We observed that simulations outcomes generally matched well with the analytical predictions when the selection coefficient is one order of magnitude larger than the baseline mutation rate (e.g., recall the first paragraph of section 2.3).

Three main results can be drawn from eqs. (20)–(21) and Fig. 2. First, selection favours physiologically costly germline maintenance at the expense of lowering investment into vital rates (survival and reproduction), especially when baseline mutation rate is higher (see Fig. 2a). And as expected, investment into maintenance is higher when returns from investment into vital rates diminish more abruptly (α is smaller). Second, when germline maintenance evolves, the mutation rate ($\mu(\mathbf{u}^*)$) depends only on the scaling factors (α and α_μ) and is independent of the baseline mutation rate μ_b (see Fig. 2c and eq. 21). This is so in this model because the effect of μ_b on the cost of germline maintenance via the expected survival $\bar{s}(\mathbf{u}^*)$ cancels out due to the nature of density-dependence (decrease in expected survival is cancelled out by the increase in the expectation of acquiring a breeding spot; see eq. 18 when taking $\alpha_s = \alpha_f = \alpha$). Third, the reproduction-survival trade-off entails that a shift towards higher allocation to reproduction occurs as μ_b increases (Fig. 2b). This is so because the effect of the mutation rate on fitness is similar to that of external mortality and thus decreases the value of allocating resource to survival. As a result, reproduction is prioritised when μ_b is large. Connected to this observation, we find that immortality (complete survival, $\bar{s}(\mathbf{u}^*) = s_0(\mathbf{u}^*) = 1$) can evolve only in the absence of external mortality ($s_b = 1$) and zero baseline mutation rate ($\mu_b = 0$, see eq. (20)). In section 1.1.4. of S.I., we numerically checked that our results are qualitatively robust when relaxing the assumption that the scaling factors of investment into reproduction and survival are not equal $\alpha_f \neq \alpha_s$.

3.2 Coevolution of age at maturity and germline maintenance

3.2.1 Biological scenario

Our second scenario is about the evolution of the time at maturity when mutation accumulation can occur during growth and reproduction. To that end, we consider that age is continuous and each individual undergoes the following events. (1) An individual is born and grows in size until it reaches maturity (growth phase). (2) At maturity an individual starts to reproduce at a constant rate and fecundity is assumed to be density dependent (reproductive phase). (3) Throughout their lives individuals die at some constant rate and acquire mutations. We postulate that individuals have again a life-history trait consisting of two components $\mathbf{u} = (u_g, u_m)$, where u_g is the allocation to germline maintenance (lowering the mutation rate) and u_m is the age-at-maturity. The life-history trait \mathbf{u} determines how resources are allocated between three physiological functions: (i) a proportion u_g of resources is allocated to maintenance of the germline at any age a , (ii) a proportion $(1 - u_g)$ of resources are allocated to growth when an individual is of age $a < u_m$, (iii) a proportion $(1 - u_g)$ of resources is allocated to reproduction when an individual is at age $a \geq u_m$, (hence $\mathbf{u} \in \mathcal{U}[\mathcal{J}] = [0, 1]^2$).

We assume that an individual with trait \mathbf{u} and i deleterious mutations in a population with resident trait \mathbf{v} has birth, death, and mutation rate throughout lifespan given by

$$\begin{aligned}\tilde{b}_i(\mathbf{u}, \mathbf{v}) &= \tilde{b}_0(\mathbf{u}, \mathbf{v}) - i\sigma_b \quad \text{if age } a \geq u_m, \text{ zero otherwise} \\ d_i &= d_b + i\sigma_d \\ \mu(u_g) &\equiv \mu_s(u_g) = \mu_b(1 - u_g)^{\alpha_\mu},\end{aligned}\tag{22}$$

where σ_b and σ_d are, respectively, the effects on birth and death from carrying deleterious mutations, which are assumed to act additively. The death rate of an individual of the least-loaded class is determined by the baseline death rate d_b and the birth rate of such an individual is assumed to be given by

$$\tilde{b}_0(\mathbf{u}, \mathbf{v}) = \underbrace{B(x_m(\mathbf{u}))}_{b_0(\mathbf{u}, \mathbf{v})} (1 - u_g^{\alpha_b}) (1 - \gamma N(\mathbf{v})) \exp(-\mu_f),\tag{23}$$

where $B(x_m(\mathbf{u}))$ is the surplus energy rate, i.e., rate of energy available to considered life-history functions. This depends on the size $x_m(\mathbf{u})$ of the individual at maturity. Here, $(1 - u_g^{\alpha_b})$ represents how reproduction depends on the allocation strategy and $u_g^{\alpha_b}$ represents the cost to reproduction when allocating a proportion u_g of resources to germline maintenance. The parameter α_b is a scaling factor ($\alpha_b > 1$ correspond to diminishing returns of investing resources into reproduction). The term $(1 - \gamma N(\mathbf{v}))$ accounts for density-dependent regulation of reproduction, where $N(\mathbf{v})$ is the total population size of the resident population and γ tunes the intensity of density dependence. Finally, $\exp(-\mu_f)$ is the probability that the offspring do not acquire new mutations during reproduction where the mutation rate at giving birth μ_f is assumed constant. In order to close the expression for the birth rate, we need an explicit expression for

size at maturity $x_m(\mathbf{u})$. During the growth phase, we postulate that size follows the differential equation

$$\dot{x}(t) = \beta B(x(t))(1 - u_g^{\alpha_b}) \quad \text{with i.c. } x(0) = x_0, \quad (24)$$

where $B(x(t))$ is the surplus energy rate and $(1 - u_g^{\alpha_b})$ represents the proportional allocation of resources devoted towards growth (instead of repair). For tractability, we assume that $(1 - u_g^{\alpha_b})$ has the functional form as the proportional allocation towards reproduction (eq. 23) and β allows to tune how much resources are needed to grow one unit, compared to the resources needed to produce one offspring. We assume that the surplus energy rate is given by the power law $B(x(t)) = ax(t)^c$, which is considered to be appropriate for modelling size/age-at-maturity under determinate growth (see Day and Taylor (1996) for a justification). It follows from integrating eq. (24) that the size at maturity takes the form

$$x_m(\mathbf{u}) = \left(\beta a (1 - c) (1 - u_g^{\alpha_b}) u_m + x_0^{1-c} \right)^{\frac{1}{1-c}}. \quad (25)$$

In the absence of mutation rate, the model reduces to the standard model of age-at maturity (Kozłowski, 1992; Day and Taylor, 1997; Stearns, 1992; Roff, 2008). The model thus combines an unexplored trade-offs between life-history traits (growth and reproduction) and immutability (germline maintenance and repair).

3.2.2 Basic reproductive number

For this model there is also no definite end to lifespan (and so $T \rightarrow \infty$) and using eq. (9) with the life-cycle assumptions entails that the basic reproductive number of the least-loaded class reduces to

$$\tilde{R}_0(\mathbf{u}, \mathbf{v}) = \tilde{b}_0(\mathbf{u}, \mathbf{v}) \int_{u_m}^{\infty} \tilde{l}_0(a, \mathbf{u}, \mathbf{v}) da, \quad (26)$$

where $\tilde{l}_0(a, \mathbf{u}, \mathbf{v}) = \exp(-(\mu(u_g) + d_b)a)$. Substituting the expression for eq. (23) into eq. (26) and integrating yields

$$\tilde{R}_0(\mathbf{u}, \mathbf{v}) = \underbrace{B(x_m(\mathbf{u})) (1 - u_g^{\alpha_b}) \exp(-\mu_f)}_{F_1(\mathbf{u})} \times \frac{\exp(-(\mu(u_g) + d_b)u_m)}{\mu(u_g) + d_b} \times \underbrace{(1 - \gamma N(\mathbf{v}))}_{F_2(\mathbf{v})}. \quad (27)$$

This shows that one can again express the basic reproductive number as a product of the form $\tilde{R}_0(\mathbf{u}, \mathbf{v}) = F_1(\mathbf{u})F_2(\mathbf{v})$ and thus the optimisation principle (e.g. Metz et al., 2008) applies also in this model. This means that evaluating $N(\mathbf{v})$ explicitly is not needed to ascertain uninvasibility (and uninvasibility will again imply convergence stability for this model). We will nevertheless work it out and in order to derive an explicit expression for $N(\mathbf{v})$ it suffices to note that in a monomorphic resident population at a joint demographic and genetic equilibrium, each individual belonging to the least-loaded class must leave on

average one descendant with zero new mutations. Hence $\tilde{R}_0(\mathbf{v}, \mathbf{v}) = 1$ implies that at the population size at the demographic steady state is

$$N(\mathbf{v}) = \frac{B(x_m(\mathbf{v}))(1 - v_g^{\alpha_b}) - (d_b + \mu(v_g)) \exp(\mu_f + (\mu(v_g) + d_b)v_m)}{\gamma B(x_m(\mathbf{v}))(1 - v_g^{\alpha_b})}, \quad (28)$$

which holds regardless of the effects of deleterious mutations on the vital rates. This is a demographic representation and generalisation of the surprising simple result noted for unstructured semelparous populations of constant size that the nature of epistasis of deleterious mutations has no effect on the genetic load (Kimura and Maruyama, 1966; Gillespie, 2004).

3.2.3 Uninvadable and convergence stable strategies

Let us now ascertain the strategies favored by long-term evolution. Using eq. (27) along with eq. (25), taking the derivative with respect to u_g , and rearranging using the property that $\tilde{R}_0(\mathbf{v}, \mathbf{v}) = 1$, we find that the selection gradient on maintenance can be written as

$$\left. \frac{\partial \tilde{R}_0(\mathbf{u}, \mathbf{v})}{\partial u_g} \right|_{\substack{u_m=v_m \\ u_g=v_g}} = \frac{\alpha_\mu \mu(v_g)}{(1 - v_g)} \left(v_m + \frac{1}{\mu(v_g) + d_b} \right) - \alpha_b v_g^{\alpha_b - 1} \left(\beta \frac{c v_m B(x_m(\mathbf{v}))}{x_m(\mathbf{v})} + \frac{1}{(1 - v_g^{\alpha_b})} \right), \quad (29)$$

where the two terms display the trade-off between allocating resources into maintenance vs. growth and reproduction. The first term is the marginal benefit of investing into maintenance and the second term is the marginal cost of investing into maintenance, which is a weighted sum of expected loss in growth and reproduction. We find that the selection gradient on the age-at-maturity can be written as

$$\left. \frac{\partial \tilde{R}_0(\mathbf{u}, \mathbf{v})}{\partial u_m} \right|_{\substack{u_m=v_m \\ u_g=v_g}} = c \times \frac{\beta (1 - v_g^{\alpha_b}) B(x_m(\mathbf{v}))}{x_m(\mathbf{v})} - (\mu(v_g) + d_b). \quad (30)$$

The first term is the marginal benefit of investment into growth and thus the benefit for maturing later, while the second terms is the marginal cost of investment into growth and thus the benefit for maturing earlier. We can see that the increase in mutation rate will select for earlier age-at-maturity.

By first solving $\partial \tilde{R}_0(\mathbf{u}, \mathbf{v}) / \partial u_m = 0$ for u_m^* when evaluated at $\mathbf{v} = \mathbf{u} = \mathbf{u}^*$, we obtain

$$u_m^*(u_g^*) = \frac{1}{1 - c} \times \left(\frac{c}{d_b + \mu(u_g^*)} - \frac{x_0}{\beta [1 - (u_g^*)^{\alpha_b}] B(x_0)} \right), \quad (31)$$

which is a function u_g^* . Eq. (31) says that individuals tend to mature later, when individuals growth rate at birth $\dot{x}(0)$ ($= \beta [1 - (u_g^*)^{\alpha_b}] B(x_0)$) is higher and/or when death rate d_b , mutation rate $\mu(u_g^*)$, and birth size x_0 are smaller (holding everything else constant). When $\mu_b \rightarrow 0$ and $u_g^* \rightarrow 0$, age-at-maturity reduces to $u_m^* = (1 - c)^{-1} [c/d_b - x_0 / [\beta a x_0^c]]$, which is consistent with standard results about the optimal age/size at maturity (see e.g. Day and Taylor, 1996) and it is useful to compare how allocation to germline maintenance affects the age-at-maturity. In order to determine the joint equilibrium $\mathbf{u}^* = (u_m^*, u_g^*)$, we

need to substitute eq. (31) into eq. (30) and solve for u_m^* and u_g^* at $\mathbf{v} = \mathbf{u}^*$. We were unable to obtain an analytical solution for the general case. But restricting attention to $\alpha_\mu = \alpha_b = 2$ (i.e. assuming diminishing returns of investment into germline maintenance and reproduction), we find that

$$\begin{aligned} u_g^* &= \frac{2\mu_b + d_b - \sqrt{d_b(d_b + 4\mu_b)}}{2\mu_b} \\ u_m^* &= \frac{1}{(1-c)} \times \left[c \left(\frac{\sqrt{d} + \sqrt{d_b + 4\mu_b}}{2d_b\sqrt{d_b + 4\mu_b}} \right) - \frac{x_0}{\beta c B(x_0)} \left(\frac{d_b + 2\mu_b + \sqrt{d_b(d_b + 4\mu_b)}}{2\sqrt{d_b(d_b + 4\mu_b)}} \right) \right] \end{aligned} \quad (32)$$

with corresponding mutation rate given by

$$\mu(u_g^*) = \frac{(d_b - \sqrt{d_b}\sqrt{d_b + 4\mu_b})^2}{4\mu_b}, \quad (33)$$

while the corresponding population size $N(\mathbf{u}^*)$ can also be explicitly expressed in terms of parameters but remains complicated (see section 2.1.4. in S.I. for the full expression).

We checked that for biologically realistic parameter values, the equilibrium $\mathbf{u}^* = (u_g^*, u_m^*)$ (see Fig. 4 panels (a) and (b) for graphical depiction of the equilibrium as a function of the baseline mutation rate) determined by eq. (32) is uninvadable and convergence stable (e.g. for the parameter values in Fig. 4 and see section 2.5.4. and 2.5.5. in S.I.). Further, using individual-based stochastic simulations, we were able to confirm that $\mathbf{u}^* = (u_g^*, u_m^*)$ given in eq. (32) is indeed as stable attractor of the evolutionary dynamics (see Fig. 5 for a graphical depiction of convergence in the individual-based simulations for four different initial population states). Fig. (4) also illustrates the equilibrium population size $N(\mathbf{u}^*)$ (panel c), and the uninvadable mutation rate $\mu(u_g^*)$ (panel d) as a function of the baseline mutation rate μ_b . Fig. (6) illustrates the body size at maturity $x_m(\mathbf{u}^*)$ (panel a) and the effective birth rate $\tilde{b}_0(\mathbf{u}^*, \mathbf{u}^*)$ at the uninvadable population state as a function of baseline mutation rate. Overall, Fig. (4) demonstrates, again, that the analytically obtained results (here using eqs. 32–33) correspond very closely to those obtained by carrying out individual-based simulations of the full process (see section 2.3. in S.I. file for the Mathematica code).

Three main results can be drawn from eqs. (32)–(33) and Figs. 4 and 6. First, as in the previous example, selection favours physiologically costly germline maintenance at the expense of lowering the investment into life-history functions (here, into growth and reproduction, see Fig. 4a). Also, the uninvadable mutation rate ($\mu(\mathbf{u}^*)$) monotonically increases with the baseline mutation rate (Fig. 4d). Second, we find that an earlier age at maturity and onset of reproduction compared to the standard life-history prediction, especially when baseline mutation rate is high (Fig. 4b). This stems from the fact that, as in the previous model, the mutation rate and the external mortality have a qualitatively similar effect on fitness by decreasing effective survival of gene transmission and thus have the same effect on the growth-reproduction trade-off. This can be observed mathematically, as the marginal cost of investment into growth is given by $(\mu(v_g) + d_b)$ (see the last term in eq. 30. For this reason we find that the shift in growth-reproduction trade-off towards reproduction is higher under: (i) high external mortality rates and

(ii) high baseline mutation rates. Since maturing earlier causes the growth period to be shorter, the body size at maturity $x_m(\mathbf{u}^*)$ will also be smaller with higher baseline mutation rate μ_b (Fig. 6a). Smaller body size at maturity, in turn, causes the birth rate $b_0(\mathbf{u}^*, \mathbf{u}^*)$ to be smaller (Fig. 6b). Third, higher baseline mutation rate causes smaller equilibrium population size (Fig. 4c), which is a known result in population genetics (see e.g. Gabriel et al., 1993). In summary, we thus find that factors that increase the baseline mutation rate cause higher investment into reproduction at the expense of smaller size and earlier age at maturity, higher uninventable mutation rate, and lower equilibrium population size.

4 Discussion

Our formalisation of the long term coevolution between life-history and deleterious mutation accumulation shows that an evolutionary invasion analysis of this process is tractable when the deleterious mutation rate is not too high so that the least-loaded class dominates in frequency the resident population. Then, the basic reproductive number of the least-loaded class (eq. 6 and eq. 9) allows to characterise the joint evolutionary stable life-history and deleterious mutation rate under a wide range of biological scenarios under asexual reproduction in age- and physiologically-structured populations. We analysed two specific scenarios to illustrate this invasion analysis approach: (i) coevolution between reproductive effort and the mutation rate and (ii) coevolution between the age-at-maturity and the mutation rate. These two models confirmed the validity of using the least-loaded class as a fitness proxy by comparing results to those obtained by individual-based stochastic simulations (Figs. 2–4) and provide a number of insights about life-history and deleterious mutation accumulation coevolution.

The model for the coevolution of reproductive effort with the mutation rate shows that positive deleterious mutation rate evolves when selection against increasing the mutation rate is balanced by the cost of germline maintenance and thus extends the well-known results from population genetics (Kimura, 1967; Kondrashov, 1995; Dawson, 1998, 1999) to an explicit life-history theory context. Here, we find that the life-history resource allocation trade-off between reproduction and survival entails a shift towards more allocation of resources to reproduction under high baseline mutation rate. This extends to evolving mutation rate, the result of Charlesworth (1990) obtained from a numerical model that a higher level of a fixed mutation rate (no germline maintenance) causes higher allocation to reproduction over survival. We predict that the shift in survival-reproduction trade-off towards reproduction is stronger under: (i) the conditions when converting resources into vital rates exhibits more abrupt diminishing returns (e.g. for environments, where organisms have high maintenance costs, e.g. colder climates), (ii) high external mortality rates (e.g. high predation environment), and (iii) high baseline mutation rates (e.g. induced by environmental stressors). We also find that immortality (complete survival) cannot evolve even in an environment with no external mortality because mutation rate cannot be brought down to zero. This highlights the less appreciated role of mutation accumulation, in addition to the extrinsic, environmentally caused hazards, that prevent the evolution of immortality (Medawar, 1952; Hamilton, 1966; Charlesworth, 1994). This means that the forces of selection on survival and reproduction (Hamilton, 1966; Ronce and

Promislow, 2010) also decline due to mutation rate. Overall, this example reveals that endogenous and/or exogenous factors that increase baseline mutation rate cause lower lifespans through higher allocation to fecundity, while the observed mutation rate remains constant.

The model for the coevolution of age-at-maturity and the mutation rate similarly yields that positive mutation rate is evolutionarily stable, but here germline maintenance trades off against investment into growth and reproduction. This extends the observation of Dańko et al. (2012) from a numerical model that looked at the effect of fixed mutation rate on the age-at maturity. They found that higher fixed mutation rate (no germline maintenance) causes earlier age-at-maturity, but they concluded that this effect would be relatively small and would be observable only under extreme conditions. Here, we show that mutation rate can significantly affect life-history trade-offs, since allocation to germline maintenance co-evolves with life-history. We predict that higher mutation rates are expected to be correlated with smaller body size at maturity (earlier switch to reproduction) and lower equilibrium population size. Increased baseline mutation rate thus increases the effect of drift and when the population size is small enough the force of drift can no longer be ignored (Lynch et al., 2016), which can eventually lead to a positive feedback between drift and mutation accumulation, i.e. mutational meltdown of the (asexual) population (Gabriel et al., 1993). Our simulations show, however, that even for a population of about 2000 individuals, drift does not significantly affect the predictions of our model (see Fig. 4). Using individual-based simulations, the coevolution between somatic maintenance, germline maintenance, body size at maturity, and population size has been explored by (Rozhok and DeGregori, 2019) where they found that selection for higher body size (by imposing size-dependent mortality) can lead to higher germline mutation rate because more resources need to be invested into somatic maintenance. Thus, they found that higher germline mutation rate and body size at maturity are expected to be negatively correlated (an opposite prediction from our result). It is however unclear what is driving the selection towards higher somatic maintenance at the expense of germline maintenance in their model and the generality of their simulations needs to be further studied.

The analysis of these two models suggests two findings about how life-histories co-evolve with deleterious mutation rates. First, the trade-off between lowering the rate of mutations vs investing into life-history functions affect the evolutionary outcome of life-history trade-offs (e.g. survival-vs-reproduction or growth-vs-reproduction). Hence, mutation accumulation can have a significant effect on life-history evolution through the process of coevolution that previous models focusing on the effect of fixed mutation rates on life-history evolution have not revealed (Charlesworth, 1990; Dańko et al., 2012). Looking at the effect of fixed mutation rates on life-history evolution underestimates the effect of deleterious mutation accumulation on life-history evolution, as it does not take into account the effect of the physiological cost of immutability on life-history evolution. Second, factors that contribute to higher baseline mutation rate select for “faster” life-histories: higher investment into current reproduction at the expense of survival and earlier age-at-maturity. Factors that could increase the baseline mutation rate μ_b include factors that increase DNA replications errors (number of germ-line cell divisions) or environmental mutagens

(oxygen level, nutrition quality, see e.g. Ferenci, 2019 for a review).

In conclusion, the physiological cost of lowering the mutation rate connects life-history trade-offs and (deleterious) mutation accumulation. Studying the evolution of the interaction between life history and mutation rate can enrich the understanding of diverse array of biological phenomena from the evolution of ageing to patterns of mutation rate evolution. Our hope is that the formalisation proposed here can be fruitfully used to this end.

Appendix A: Continuous time invasion process with mutation accumulation

In section (2.2.2), we presented the renewal equation and growth rate for a discrete time process (eqs. 2–8). Let us now consider that time is continuous and that age-structure is likewise continuous so that $\mathcal{T} = [0, \infty)$. For this case, accounting entails that the expected number $n_i(t)$ of individuals at time t that descend from a single newborn (age class zero) ancestor residing at $t = 0$ in class \mathcal{C}_i satisfies

$$n_i(t) = \tilde{l}_i(t) + \int_0^t n_i(t-a) \tilde{b}_i(a) \tilde{l}_i(a) da, \quad (\text{A.1})$$

where all quantities maintain the same interpretation as in the discrete time case.

Eq. (A.1) is functionally equivalent to the standard renewal equation of population dynamics for continuous age-structured populations (Charlesworth, 1994, eq. 1.41). As such, and as for the discrete time case, it then follows from the standard results of population dynamic processes in age-structured populations (Charlesworth, 1994, p. 27) that asymptotically, as $t \rightarrow \infty$, the number $n_i(t)$ grows geometrically as

$$n_i(t) \sim \rho_i^t K_i, \quad (\text{A.2})$$

where K_i is some constant depending on the process and $\rho_i = \exp(r_i)$, where r_i is the mutant growth rate (or Malthusian parameter), which is the unique root of the Euler-Lotka equation

$$\int_0^\infty \exp(-ar_i) \tilde{b}_i(a) \tilde{l}_i(a) da = 1. \quad (\text{A.3})$$

Appendix B: Description of individual-based simulations

We here describe how we carried out the individual-based (stochastic) simulations used for the two model examples in the main text. The simulation algorithms scrupulously implement the life-cycle assumption of these models with the only differences relative to the analytical model being that (i) population size is finite and (ii) the mutation rate at the life-history locus is positive $\mu_{LH} > 0$ (but kept small) in the simulations. This makes the coevolutionary process in the simulations irreducible (see also discussion section 2.3) and subject to genetic drift.

The simulation algorithm for the ‘‘Coevolution of reproductive effort and mutation rate’’ scenario (see section 1.3. of S.I for the Mathematica code) follows a population composed of a finite and fixed number (=7500 in the simulations) of individuals, where each individual is described by its genetic state (vector of traits consisting of allocation to maintenance, allocation to survival and number of deleterious mutations the individual has). One life-cycle iteration then proceeds as follows. We start by computing the fecundity of each adult individual, which is determined by its trait values (eq. (11)). Then, we evaluate the survival probability of each adult individual according to its trait values (the survival of an individual is given by a Bernoulli random variable with mean given by its survival probability eq. (11)). After eliminating the

dead individuals, we fill the “vacated breeding spots” by randomly sampling offspring from the relative fecundity of all adult individuals before survival, thus effectively implementing a Wright-Fisher process for reproduction (Mode and Gallop, 2008). Once a newborn is chosen to fill the breeding spot, each of its traits mutate independently with probability ($\mu_{LH} = 0.01$ in our actual simulations). The effect size of a mutation follows a Normal distribution with zero mean and a standard deviation ($=0.02$ in our simulations). Finally, we allow for deleterious mutations to accumulate at the deleterious mutation locus according to a Poisson distribution with mean that depends on the life-history locus (as specified by eq. (11)). To obtain the results shown in 2, we initialised the simulation with a monomorphic population, with no deleterious mutations and life-history trait values given by the analytically predicted equilibrium. In Fig. 3 we demonstrate the convergence stability of our simulations and we started the simulations away from the equilibrium for four different initial values of the traits.

The simulation algorithm for the “Coevolution of age of maturity and germline maintenance” scenario (see section 2.3. of S.I for the Mathematica code) follows a population whose size is endogenously determined according to a continuous-time stochastic updating process using the so-called “thinning” algorithm described in Section 3.1 of Ferriere and Tran (2009), which allows to exactly implement our life-cycle assumptions. A thinning algorithm is essentially an algorithm to simulate the points in an inhomogeneous Poisson process (inhomogeneous Poisson processes can be simulated by “thinning” the points from the homogeneous Poisson process), where the points or events take place sequentially (see e.g. Chen, 2016 for a conceptual description). Hence, under this algorithm, each individual is described by a vector specifying its age, allocation to repair, the age at maturity, and the number of deleterious mutations the individual has. The events in the thinning algorithm then follow a Poisson point process whose mean is determined by the vital rates (eq. (22)) and where the occurrence of the events depends on the relative weights set by birth, death, and mutation rates of an individual. We defined as a “generation” $N(\mathbf{u}^*)$ iterations of the thinning algorithm, where $N(\mathbf{u}^*)$ is the analytical prediction of the carrying capacity of the model. This is so because during one iteration of the thinning algorithm, a maximum of one event can occur (birth, death, or mutation of an individual) to one randomly chosen individual and so after having iterated the process $N(\mathbf{u}^*)$ times, on average the total population has been sampled. Thus, in order to produce a single data point in Fig. 4, we ran the six million ($=N(\mathbf{u}^*) \times N_{\text{generations}} \approx 2000 \times 3000$) iterations of the thinning algorithm. The mutation rate in the life-history locus is set to $\mu_{LH} = 0.1$ and the effect size of the mutation follows a Normal distribution with zero mean and a standard deviation ($=0.07$ in our simulations). Simulating the results shown in 4, we initialised the simulation with a monomorphic population, where individual age is given by $a = 1/d_b$ (recall, that d_b is the baseline mortality, with no deleterious mutations and life-history trait values given by the analytically predicted equilibrium. In Fig. 5 we demonstrate the convergence stability of our simulations and we started the simulations away from equilibrium for four different initial values of the traits.

References

- Altenberg, L. 2009. The evolutionary reduction principle for linear variation in genetic transmission. *Bull. Math. Biol.* 71:1264–1284.
- Altenberg, L., U. Liberman, and M. W. Feldman. 2017. Unified reduction principle for the evolution of mutation, migration, and recombination. *Proc. Natl. Acad. Sci. U.S.A.* 114:E2392–E2400.
- André, J.-B., and B. Godelle. 2006. The evolution of mutation rate in finite asexual populations. *Genetics* 172:611–626.
- Avila, P., L. Fromhage, and L. Lehmann. 2019. Sex-allocation conflict and sexual selection throughout the lifespan of eusocial colonies. *Evolution* 73:1116–1132.
- Avila, P., T. Priklopil, and L. Lehmann. 2021. Hamilton’s rule, gradual evolution, and the optimal (feedback) control of phenotypically plastic traits. *J. Theor. Biol.* 526:110602.
- Baumdicker, F., E. Sester-Huss, and P. Pfaffelhuber. 2020. Modifiers of mutation rate in selectively fluctuating environments. *Stoch. Process. Their. Appl.* 130:6843–6862.
- Bürger, R. 2000. *The Mathematical Theory of Selection, Recombination, and Mutation*. John Wiley and Sons, New York.
- Case, T. J. 2000. *An Illustrated Guide to Theoretical Ecology*. Oxford University Press, Oxford.
- Caswell, H. 2000. *Matrix Population Models*. Sinauer Associates, Massachusetts.
- Charlesworth, B. 1990. Optimization models, quantitative genetics, and mutation. *Evolution* 44:520–538.
- . 1994. *Evolution in Age-Structured Populations*. 2nd ed. Cambridge University Press, Cambridge.
- Charnov, E. L. 1993. *Life history invariants: some explorations of symmetry in evolutionary ecology*. Oxford University Press, New York.
- Chen, H.-y., C. Jolly, K. Bublys, D. Marcu, and S. Immler. 2020. Trade-off between somatic and germline repair in a vertebrate supports the expensive germ line hypothesis. *Proc. Natl. Acad. Sci. U.S.A.* 117:8973–8979.
- Chen, Y. 2016. *Thinning algorithms for simulating point processes*. Florida State University, Tallahassee, FL .
- Cichon, M., and J. Kozłowski. 2000. Ageing and typical survivorship curves result from optimal resource allocation. *Evol. Ecol. Research* 2:857–870.
- Dańko, M. J., J. Kozłowski, J. W. Vaupel, and A. Baudisch. 2012. Mutation accumulation may be a minor force in shaping life history traits. *PLoS One* 7:e34146.
- Dawson, K. J. 1998. Evolutionarily stable mutation rates. *J. Theor. Biol.* 194:143–157.
- . 1999. The dynamics of infinitesimally rare alleles, applied to the evolution of mutation rates and the expression of deleterious mutations. *Theor. Popul. Biol.* 55:1–22.
- Day, T., and P. D. Taylor. 1996. Evolutionarily stable versus fitness maximizing life histories under frequency-dependent selections. *Proc. R. Soc. B: Biol. Sci.* 263:333–338.
- . 1997. Hamilton’s rule meets the Hamiltonian: Kin selection on dynamic characters. *Proc. R. Soc. B: Biol. Sci.* 264:639–644.
- . 2000. A generalization of Pontryagin’s maximum principle for dynamic evolutionary games among relatives. *Theor. Popul. Biol.* 57:339–356.
- de Roos, A. M. 1997. A gentle introduction to models of physiologically structured populations. *In* S. Tuljapurkar and H. Caswell, eds., *Structured-Population Models in Marine, Terrestrial, and Freshwater Systems*. Chapman & Hall, New York.

- Dercole, F., and S. Rinaldi. 2008. *Analysis of Evolutionary Processes: The Adaptive Dynamics Approach and Its Applications*. Princeton University Press, Princeton, NJ.
- Eigen, M. 1971. Selforganization of matter and the evolution of biological macromolecules. *Naturwissenschaften* 58:465–523.
- Eshel, I. 1983. Evolutionary and continuous stability. *J. Theor. Biol.* 103:99–111.
- . 1996. On the changing concept of evolutionary population stability as a reflection of a changing point of view in the quantitative theory of evolution. *J. Math. Biol.* 34:485–510.
- Eshel, I., and M. W. Feldman. 1984. Initial increase of new mutants and some continuity properties of ess in two-locus systems. *Am. Nat.* 124:631–640.
- Eshel, I., and U. Motro. 1988. The three brothers’ problem: kin selection with more than one potential helper. 1. the case of immediate help. *Am. Nat.* 132:550–566.
- Eyre-Walker, A., and P. D. Keightley. 2007. The distribution of fitness effects of new mutations. *Nature Reviews Genetics* 8:610–618.
- Ferenci, T. 2019. Irregularities in genetic variation and mutation rates with environmental stresses. *Environ. Microbiol.* 21:3979–3988.
- Ferrière, R., and M. Gatto. 1995. Lyapunov exponents and the mathematics of invasion in oscillatory or chaotic populations. *Theor. Popul. Biol.* 48:126–171.
- Ferriere, R., and V. C. Tran. 2009. Stochastic and deterministic models for age-structured populations with genetically variable traits. Pages 289–310 in *ESAIM: Proceedings*. Vol. 27. EDP Sciences.
- Frank, S. A. 2008. All of life is social. *Curr. Biol.* 16:R648–R650.
- Gabriel, W., M. Lynch, and R. Bürger. 1993. Muller’s ratchet and mutational meltdowns. *Evolution* 47:1744–1757.
- Geritz, S. A. H., E. Kisdi, G. Meszéna, and J. A. J. Metz. 1998. Evolutionarily singular strategies and the adaptive growth and branching of the evolutionary tree. *Evol. Ecol.* 12:35–57.
- Gerrish, P. J., A. Colato, A. S. Perelson, and P. D. Sniegowski. 2007. Complete genetic linkage can subvert natural selection. *Proc. Natl. Acad. Sci. U.S.A.* 104:6266–6271.
- Gervais, C., and D. Roze. 2017. Mutation rate evolution in partially selfing and partially asexual organisms. *Genetics* 207:1561–1575.
- Gillespie, J. H. 1981. Mutation modification in a random environment. *Evolution* pages 468–476.
- . 2004. *Population Genetics: a Concise Guide*. Johns Hopkins University Press, Baltimore, Maryland.
- Haigh, J. 1978. The accumulation of deleterious genes in a population—Muller’s ratchet. *Theor. Popul. Biol.* 14:251–267.
- Hamilton, W. D. 1966. The moulding of senescence by natural selection. *J. Theor. Biol.* 12:12–45.
- Holsinger, K. E., and M. W. Feldman. 1983. Modifiers of mutation rate: evolutionary optimum with complete selfing. *Proc. Natl. Acad. Sci. U.S.A.* 80:6732–6734.
- Irie, T., and Y. Iwasa. 2005. Optimal growth pattern of defensive organs: the diversity of shell growth among mollusks. *Am. Nat.* 165:238–249.
- Iwasa, Y. 2000. Dynamic optimization of plant growth. *Evol. Ecol. Res.* 2:437–455.
- Iwasa, Y., and J. Roughgarden. 1984. Shoot/root balance of plants: optimal growth of a system with many vegetative organs. *Theor. Popul. Biol.* 25:78–105.

- Johnson, T. 1999. Beneficial mutations, hitchhiking and the evolution of mutation rates in sexual populations. *Genetics* 151:1621–1631.
- Karlin, S., and H. M. Taylor. 1975. *A First Course in Stochastic Processes*. Academic Press, San Diego.
- . 1981. *A Second Course in Stochastic Processes*. Academic Press, San Diego.
- Kimura, M. 1967. On the evolutionary adjustment of spontaneous mutation rates. *Genet. Res.* 9:23–34.
- Kimura, M., and T. Maruyama. 1966. The mutational load with epistatic gene interactions in fitness. *Genetics* 54:1337.
- Kirkwood, B. 1986. *Accuracy in Molecular Processes: Its Control and Relevance to Living System*. Chapman and Hall, New York.
- Kondrashov, A. S. 1995. Modifiers of mutation-selection balance: general approach and the evolution of mutation rates. *Genet. Res.* 66:53–69.
- Kozlowski, J. 1992. Optimal allocation of resources to growth and reproduction: implications for age and size at maturity. *Trends Ecol. Evol.* 7:15–19.
- Lehmann, L., C. Mullon, E. Akçay, and J. Van Cleve. 2016. Invasion fitness, inclusive fitness, and reproductive numbers in heterogeneous populations. *Evolution* 70:1689–1702.
- Leigh, E. G. 1970. Natural selection and mutability. *Am. Nat.* 104:301–305.
- Leimar, O. 2009. Multidimensional convergence stability. *Evol. Ecol. Research* 11:191–208.
- León, J. A. 1976. Life histories as adaptive strategies. *J. Theor. Biol.* 60:301–335.
- Lesaffre, T. 2021. Population-level consequences of inheritable somatic mutations and the evolution of mutation rates in plants. *Proc. Royal Soc. B* 288:20211127.
- Lessard, S. 1990. Evolutionary stability: one concept, several meanings. *Theor. Popul. Biol.* 37:159–170.
- Liberman, U., and M. W. Feldman. 1986. Modifiers of mutation rate: a general reduction principle. *Theor. Popul. Biol.* 30:125–142.
- Lynch, M., M. S. Ackerman, J.-F. Gout, H. Long, W. Sung, W. K. Thomas, and P. L. Foster. 2016. Genetic drift, selection and the evolution of the mutation rate. *Nature Reviews Genetics* 17:704–714.
- Lynch, M., R. Bürger, D. Butcher, and W. Gabriel. 1993. The mutational meltdown in asexual populations. *J. Hered.* 84:339–344.
- Maklakov, A. A., and S. Immler. 2016. The expensive germline and the evolution of ageing. *Curr. Biol.* 26:R577–R586.
- Maynard Smith, J. 1982. *Evolution and the Theory of Games*. Cambridge University Press, Cambridge.
- Medawar, P. B. 1952. *An unsolved problem of biology. An Inaugural Lecture Delivered at University College, London*.
- Metz, J. A. J., S. D. Mylius, and O. Diekmann. 2008. When does evolution optimize? *Evol. Ecol. Res.* 10:629–654.
- Metz, J. A. J., R. M. Nisbet, and S. A. H. Geritz. 1992. How should we define fitness for general ecological scenarios? *Trends Ecol. Evol.* 7:198–202.
- Metz, J. A. J., K. Staňková, and J. Johansson. 2016. The canonical equation of adaptive dynamics for life histories: from fitness-returns to selection gradients and Pontryagin’s maximum principle. *J. Math. Biol.* 72:1125–1152.
- Metzger, J. J., and S. Eule. 2013. Distribution of the fittest individuals and the rate of muller’s ratchet in a model with overlapping generations. *PLoS Comput. Biol.* 9:e1003303.

- Michod, R. E. 1979. Evolution of life histories in response to age-specific mortality factors. *Am. Nat.* 113:531–550.
- Mode, C. J. 1968. A multidimensional age-dependent branching process with applications to natural selection. i. *Math. Biosci.* 3:1–18.
- . 1971. Multitype branching processes: theory and applications. 34. American Elsevier Publishing Company, New York.
- Mode, C. J., and R. J. Gallop. 2008. A review on monte carlo simulation methods as they apply to mutation and selection as formulated in wright–fisher models of evolutionary genetics. *Math. Biosci.* 211:205–225.
- Monaghan, P., and N. B. Metcalfe. 2019. The deteriorating soma and the indispensable germline: gamete senescence and offspring fitness. *Proc. R. Soc. B: Biol. Sci.* 286:20192187.
- Mullon, C., L. Keller, and L. Lehmann. 2016. Evolutionary stability of jointly evolving traits in subdivided populations. *Am. Nat.* 188:175–195.
- . 2018. Social polymorphism is favoured by the co-evolution of dispersal with social behaviour. *Nat. Ecol. Evol.* 2:132–140.
- Mullon, C., and L. Lehmann. 2019. An evolutionary quantitative genetics model for phenotypic (co)variances under limited dispersal, with an application to socially synergistic traits. *Evolution* 73:1695–1728.
- Nair, K. A., and C. J. Mode. 1971. The reducible multidimensional age-dependent branching processes. *J. Math. Anal. Appl.* 33:131–139.
- Otto, S. P., and T. Day. 2007. *A biologist’s Guide to Mathematical Modeling in Ecology and Evolution*. Princeton University Press, Princeton, NJ.
- Parker, G. A., and J. Maynard Smith. 1990. Optimality theory in evolutionary biology. *Science* 349:27–33.
- Pen, I. 2000. Reproductive effort in viscous populations. *Evolution* 54:293–297.
- Perrin, N. 1992. Optimal resource allocation and the marginal value of organs. *Am. Nat.* 139:1344–1369.
- Perrin, N., and R. M. Sibly. 1993. Dynamic models of energy allocation and investment. *Annu. Rev. Ecol. Syst.* 24.
- Priklopil, T., and L. Lehmann. 2021. Metacommunities, fitness and gradual evolution. *Theor. Popul. Biol.* 142:12–35.
- Roff, D. A. 2008. Defining fitness in evolutionary models. *J. Genet.* 87:339–348.
- Ronce, O., and D. Promislow. 2010. Kin competition, natal dispersal and the moulding of senescence by natural selection. *Proc. R. Soc. B* 277:3659–67.
- Rousset, F. 2004. *Genetic Structure and Selection in Subdivided Populations*. Princeton University Press, Princeton, NJ.
- Rozhok, A., and J. DeGregori. 2019. Somatic maintenance impacts the evolution of mutation rate. *BMC Evol. Biol.* 19:1–17.
- Schaffer, W. M. 1982. The application of optimal control theory to the general life history problem. *Am. Nat.* 121:418–431.
- Sniegowski, P. D., P. J. Gerrish, T. Johnson, and A. Shaver. 2000. The evolution of mutation rates: separating causes from consequences. *Bioessays* 22:1057–1066.
- Stearns, S. 1992. *The Evolution of Life Histories*. Oxford University Press, Oxford.

- Steinsaltz, D., S. N. Evans, and K. W. Wachter. 2005. A generalized model of mutation–selection balance with applications to aging. *Adv. Appl. Math.* 35:16–33.
- Szathmary, E., and J. Maynard Smith. 1997. From replicators to reproducers: the first major transitions leading to life. *J. Theor. Biol.* 187:555–571.
- Taylor, P. D. 1989. Evolutionary stability in one-parameter models under weak selection. *Theor. Popul. Biol.* 36:125–143.

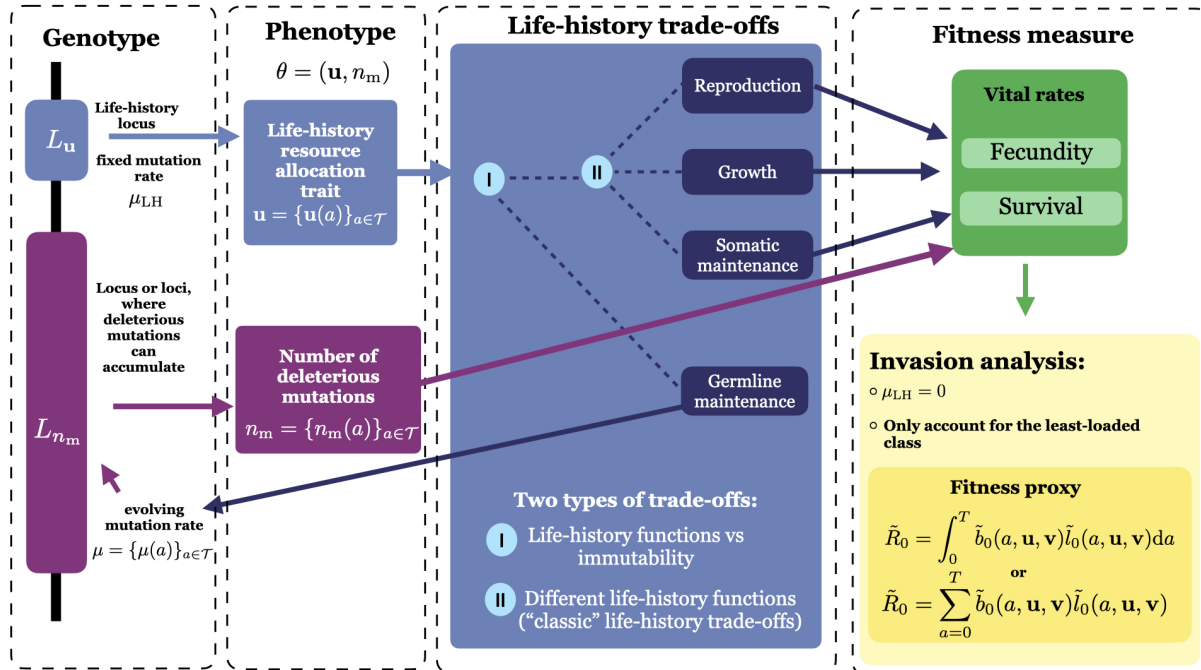


Figure 1: Key components of the life-history model with mutation accumulation. An individual's genotype is characterised by a life-history locus L_u and a deleterious mutation locus (purple rectangle) L_{n_m} . The mutation rate at the life-history locus μ_{LH} is considered to be fixed, while the mutation rate μ at the deleterious mutation locus depends on the life-history trait \mathbf{u} and is evolving. Individuals can be characterised by the life-history allocation trajectory $\mathbf{u} = \{\mathbf{u}(a)\}_{a \in \mathcal{T}}$ (life-history trait) and the number $n_m = \{n_m(a)\}_{a \in \mathcal{T}}$ of deleterious mutations accumulated in the germline throughout lifespan. The resource allocation trait captures two different types of trade-offs: (i) between immutability vs life-history and (ii) between different life-history functions themselves ("classic" life history trade-offs, e.g. Stearns, 1992; Roff, 2008). Hence, the life-history locus affects the vital rates and thus fitness directly via resource allocation to life-history functions and indirectly through allocation to germline maintenance since vital rates depend on the number of deleterious mutations. For the invasion analysis we use the basic reproductive number of the least-loaded class \tilde{R}_0 as a fitness proxy (eqs. 6 and 9 as detailed in section 2.3).

Table 1: List of key symbols of the general model.

Key symbols of the model	
a	Individual age; age a can take either discrete ($a \in \{0, 1, 2, \dots\}$) or continuous ($a \in [0, \infty]$) values over all possible age classes \mathcal{T} (e.g. $\mathcal{T} = [0, \infty]$ in many continuous age life-history models, as maximum age is often not a fixed number).
$\mathbf{u}(a)$	Individual life-history trait expressed at age a (e.g. proportional allocation fecundity, survival, germline maintenance); formally, $\mathbf{u} : \mathcal{T} \rightarrow \mathbb{R}^n$
$\mathbf{u} = \{\mathbf{u}(a)\}_{a \in \mathcal{T}}$	Full life-history schedule over all age classes (e.g. proportional allocation of resources to fecundity from birth to death); formally, $\mathbf{u} \in \mathcal{U}[\mathcal{T}]$, where $\mathcal{U}[\mathcal{T}]$ is a set of all admissible life-history schedules; namely, a set of discrete or continuous real-valued functions over domain \mathcal{T} .
$n_m(a)$	Number of deleterious mutations at age a in the locus where deleterious mutations can accumulate; formally, $n_m : \mathcal{T} \rightarrow \mathbb{N}$. Since we assume asexual reproduction, the genetic details of the locus for trait $n_m(a)$ is irrelevant (i.e. it may consist of many underlying loci).
$n_m = \{n_m(a)\}_{a \in \mathcal{T}}$	Profile of deleterious mutations across all age classes; formally, $n_m \in \mathbb{N}[\mathcal{T}]$ is an element of the space $\mathbb{N}[\mathcal{T}]$ of all possible discrete functions of range \mathbb{N} over domain \mathcal{T} .
$\mathbf{p}(\mathbf{v})$	Equilibrium probability distribution for the number of deleterious mutations in the resident population carried by individuals across the different age-classes, formally $\mathbf{p}(\mathbf{v}) \in \Delta(\mathbb{N} \times \mathcal{T})$, where $\Delta(A)$ is the set of probability measure over set A .
$\rho_0(\mathbf{u}, \mathbf{v})$	Invasion fitness (per-capita growth rate) of zero-class individuals with mutant allele \mathbf{u} in the population resident to trait \mathbf{v} ; if the least-loaded class dominates the population.
$\tilde{R}_0(\mathbf{u}, \mathbf{v})$	Basic reproductive number of the least-loaded class, i.e. the expected number of offspring with zero deleterious mutations produced by an individual with zero deleterious mutations
$\tilde{b}_0(a, \mathbf{u}, \mathbf{v})$	Effective number of newborns with zero mutations produced by zero-class mutant individuals age a in a resident population (discrete time model); effective birth rate of newborns with zero mutations of zero class mutant individual of age a in a resident population (continuous time model).
$d_0(a, \mathbf{u}, \mathbf{v})$	Death rate of zero-class mutant individual at age a in the resident population
$\tilde{l}_0(a, \mathbf{u}, \mathbf{v})$	Probability of survival of a mutant zero-class individual to age a in a resident population.
$\mu_f(a, \mathbf{u}, \mathbf{v})$	Rate at which germline mutations appear in an offspring when giving birth at age a .
$\mu_s(a, \mathbf{u}, \mathbf{v})$	Rate at which germline mutations appear in an individual at age a .

Table 2: List of key symbols of “Coevolution of reproductive effort and the mutation rate model” .

Symbols for “Coevolution of reproductive effort and the mutation rate”.	
u_g, v_g	Proportional allocation of resources to germline maintenance of mutant and resident individual, respectively.
u_s, v_s	Proportional allocation of resources to survival of mutant and resident individual, respectively.
N	Total population size; exogeneously fixed ($N = 7500$ in simulations).
f_b, s_b	Baseline (maximal) fecundity and probability of survival, respectively ($f_b = 5$, $s_b = 0.5$).
$\mu(\mathbf{u}) = \mu_s(\mathbf{u}) = \mu_f(\mathbf{u})$	Rate at which germline mutations appear in an offspring when giving birth and when surviving from generation to the next.
μ_b	Baseline mutation rate at which germline mutations appear; mutation rate, when no resources are allocated into germline maintenance.
α_f, α_s	Scaling factors of investing resources into fecundity and survival, respectively; analytical results obtained for $\alpha_f = \alpha_s = \alpha$ ($\alpha = 0.02, \alpha = 0.1, \alpha = 0.2$ in simulations).
α_μ	Scaling factor of investing resources into germline maintenance. ($\alpha_\mu = 2$).

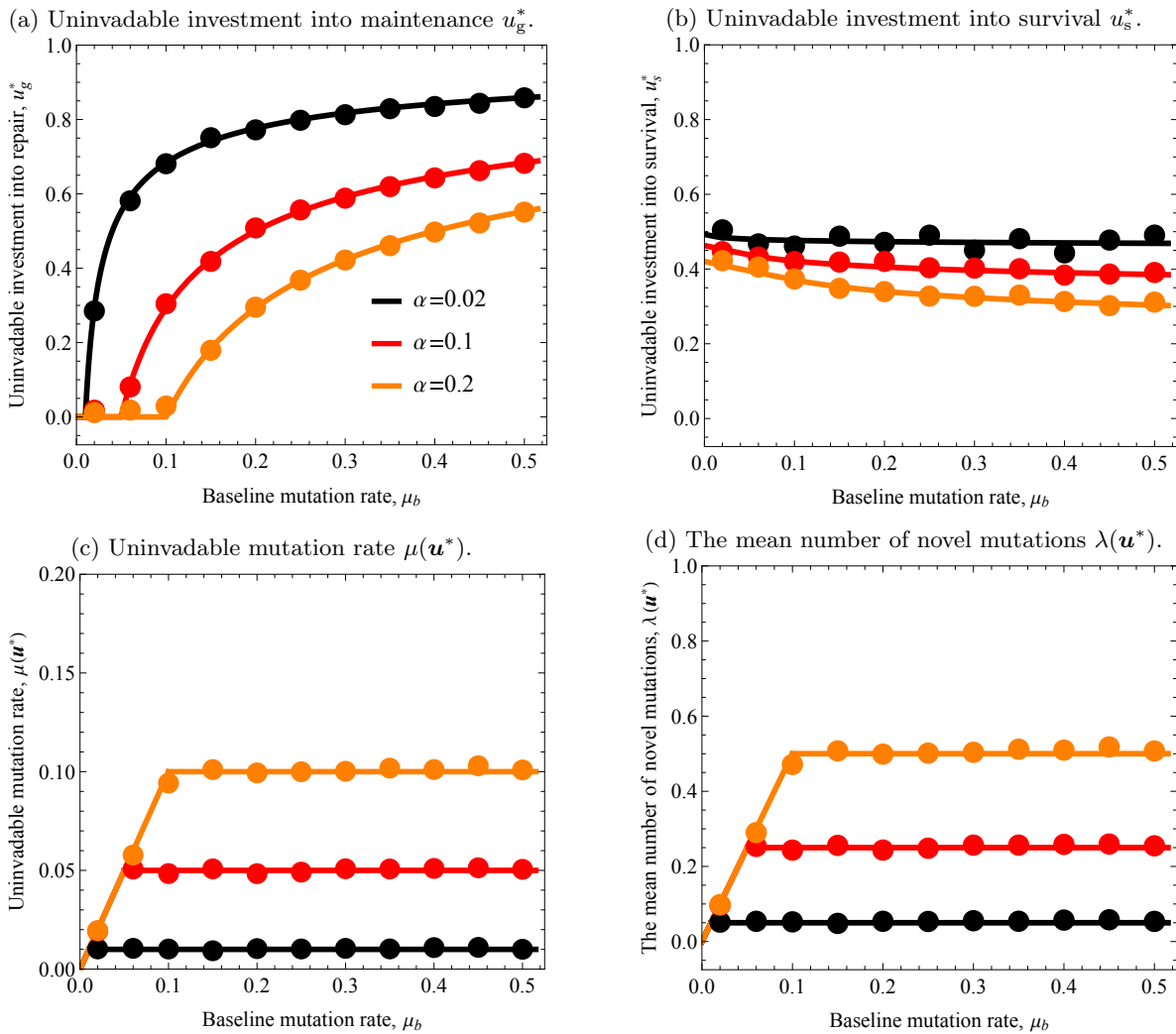


Figure 2: Predictions from the analytical model (solid lines) and from individual-based simulations of a finite population (circles) for the uninvadable life-history strategies $\mathbf{u}^* = (u_g^*, u_s^*)$ (panel a and b) and the mean number of novel mutations $\lambda(\mathbf{u}^*)$ (panel c) as functions of baseline mutation rate μ_b . The solution for the individual-based simulations are obtained as time-averages measured over 7500 generations while starting the simulation at the analytically predicted equilibrium (see Appendix B for details about the simulations and S.I. for the simulation code). The different colours represent different values of scaling factor α of reproduction and survival (smaller values of α corresponding to more strongly diminishing returns from investment into vital rates). Parameter values: $f_b = 5$, $\alpha_\mu = 2$, $s_b = 0.5$, $\sigma = \sigma_f = \sigma_s = 0.2$; for simulations: $N = 7500$, $f_b = 5$, $s_b = 0.5$.

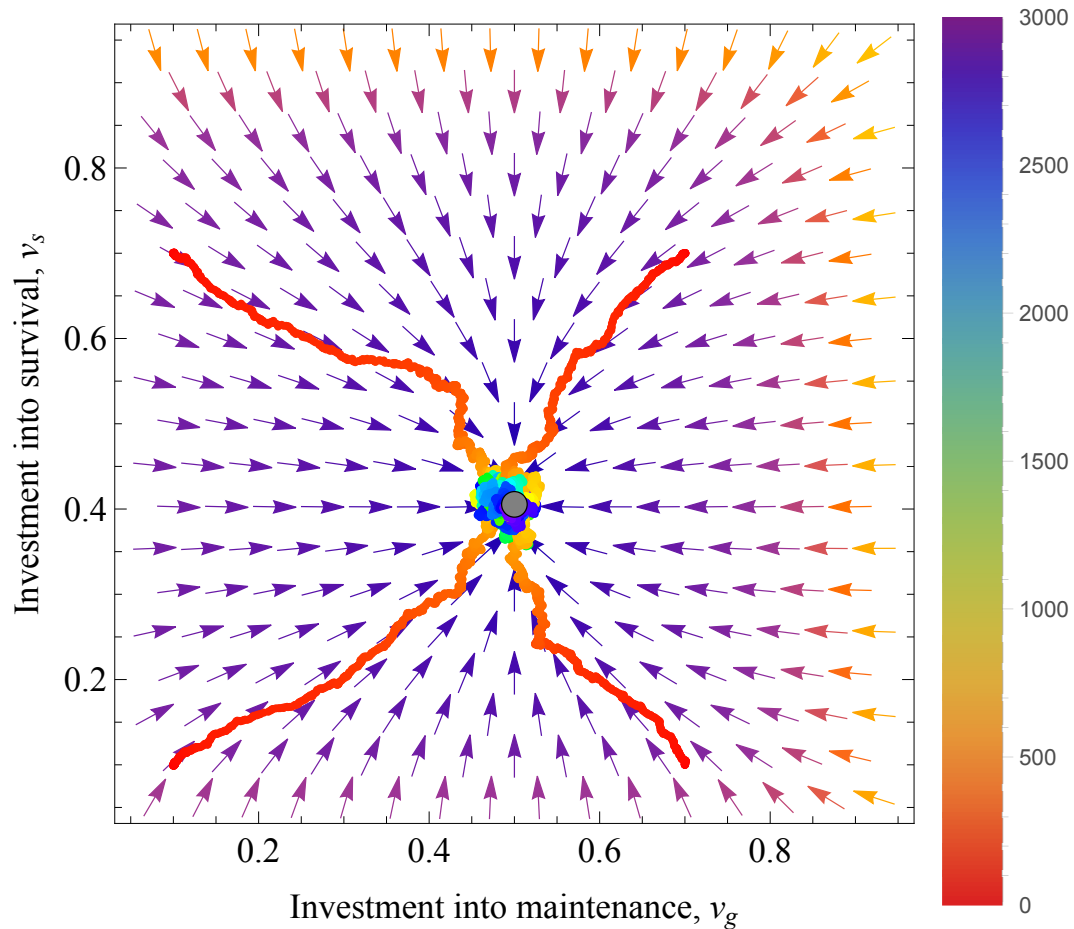


Figure 3: Evolutionary convergence towards the uninvadable life-history strategy $\mathbf{u}^* = (u_g^*, u_s^*) \approx (0.50, 0.40)$ (grey circle). The arrows give the analytic direction of selection at any population state (eqs. 18 and 19) and the colourful jagged lines represent the evolution of population average trait values over evolutionary time in simulations (from initial time, up to 3000 generations). Simulations were started from four different initial conditions: (i) $v_g = 0.1, v_s = 0.1$, (ii) $v_g = 0.1, v_s = 0.7$, (iii) $v_g = 0.7, v_s = 0.1$, and (iv) $v_g = 0.7, v_s = 0.7$. The colour of jagged lines indicates the number of generations since the start of the simulation (the color bar on the right-hand-side indicates the number of generations). The simulations indicate that the population converges close to the uninvadable strategy within 3000 generations. Parameter values: $f_b = 5, \alpha_\mu = 2, s_b = 0.5, \sigma = \sigma_f = \sigma_s = 0.2$; for simulations: $N = 6000, f_b = 5, s_b = 0.5$.

Table 3: List of key symbols of “Coevolution of age at maturity and germline maintenance model”.

Symbols for “Coevolution of age at maturity and germline maintenance model”.	
u_g, v_g	Proportional allocation of resources to germline maintenance of mutant and resident individual, respectively.
u_m, v_m	Proportional allocation of resources to germline maintenance of mutant and resident individual, respectively.
$N(\mathbf{v})$	Total population size; endogenously determined and thus depends on the resident trait \mathbf{v} .
$x(t)$	Body size of a mutant individual at age t .
$x_m(\mathbf{u})$	Body size of a mutant individual at maturity.
$B(x_m(\mathbf{u}))$	Surplus energy rate, i.e., rate of energy available to be allocated to life-history functions; we assume that the surplus energy scales as the power with size, i.e. energy available to mature individuals is $B(x_m(\mathbf{u})) = ax_m(\mathbf{u})^c$.
μ_f	Rate at which germline mutations appear in an offspring when giving birth (fixed parameter, $\mu_f = 0$ in simulations).
$\mu_s(u_g) \equiv \mu(u_g)$	Rate at which germline mutations appear in a mutant individual over time (independent of age).
μ_b	Baseline mutation rate at which germline mutations appear; mutation rate, when no resources are allocated into germline maintenance.
d_b	Baseline death rate.

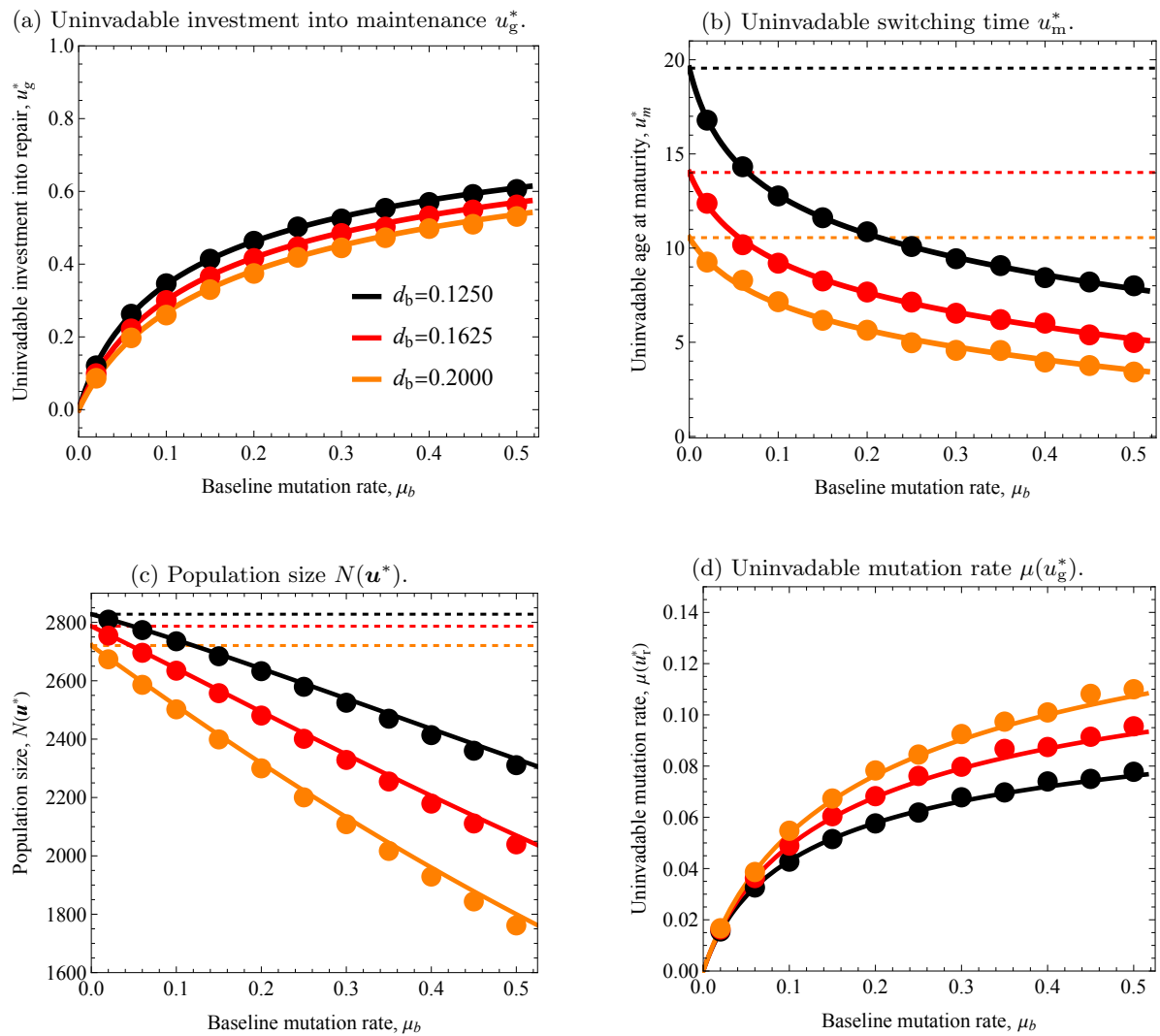


Figure 4: Predictions from the analytical model (solid lines) and from individual-based simulations (circles obtained as averages) for uninvadable life-history strategies $\mathbf{u}^* = (u_m^*, u_g^*)$ (panel a and b), population size $N(\mathbf{u}^*)$ (panel c) and mutation rate $\mu(u_g^*)$ as functions of baseline mutation rate μ_b for different values of baseline mortality d_b ($d_b = 0.1250$ - black, $d_b = 0.1625$ - red, $d_b = 0.2$ - orange). The dashed lines represent the “classical life-history” prediction (i.e. when $\mu(u_g^*) \rightarrow 0$ and $u_g^* \rightarrow 0$), where the colours of the dashed represent the different values for baseline death rate d_b parameter and match the values of solid lines ($d_b = 0.1250$ - black, $d_b = 0.1625$ - red, $d_b = 0.2$ - orange). The solution for the individual-based simulations are obtained as time-averages measured over 3000 “generations” while starting the simulation at analytically predicted equilibrium for the trait values and population size (see S.I. section 2.3 for the code and for more details). The different colours represent different values of baseline mortality rate d_b . Parameter values: $\sigma = \sigma_b = \sigma_d = 0.2$, $x_0 = 1$, $a = 0.9$, $c = 0.75$, $\gamma = 0.00035$, $\beta = 1$, $\mu_f = 0$.

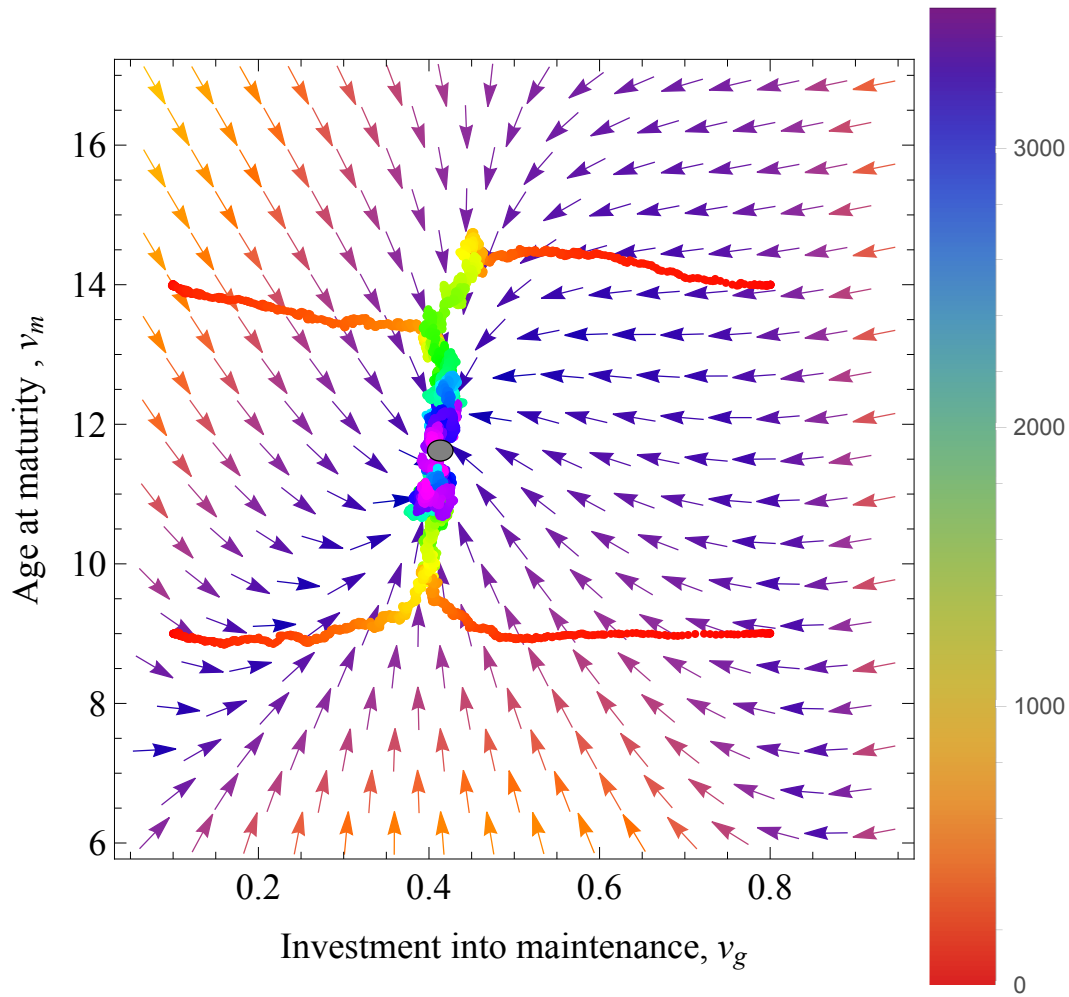


Figure 5: Evolutionary convergence to the uninvadable life-history strategy $\mathbf{u}^* = (u_g^*, u_m^*) \approx (0.41, 11.6)$ (grey circle). The arrows give the direction of selection at any resident population state (eqs. 29 and 30) and the colourful jagged lines represent the evolution of the population average trait values over evolutionary time in simulations (from initial time, up to 3500 generations). Simulations were started from four different initial conditions: (i) $v_g = 0.1, v_s = 0.1$, (ii) $v_g = 0.1, v_s = 0.7$, (iii) $v_g = 0.7, v_s = 0.1$, and (iv) $v_g = 0.7, v_s = 0.7$. The colour of jagged lines indicates the number of generations since the start of the simulation (the color bar on the right-hand-side indicates the number of generations). The simulations indicate that the population converges close to the uninvadable strategy within 3500 generations. Parameter values: $\sigma = \sigma_b = \sigma_d = 0.2, x_0 = 1, a = 0.9, c = 0.75, \gamma = 0.00035, \beta = 1, \mu_f = 0, d_b = 0.1250$.

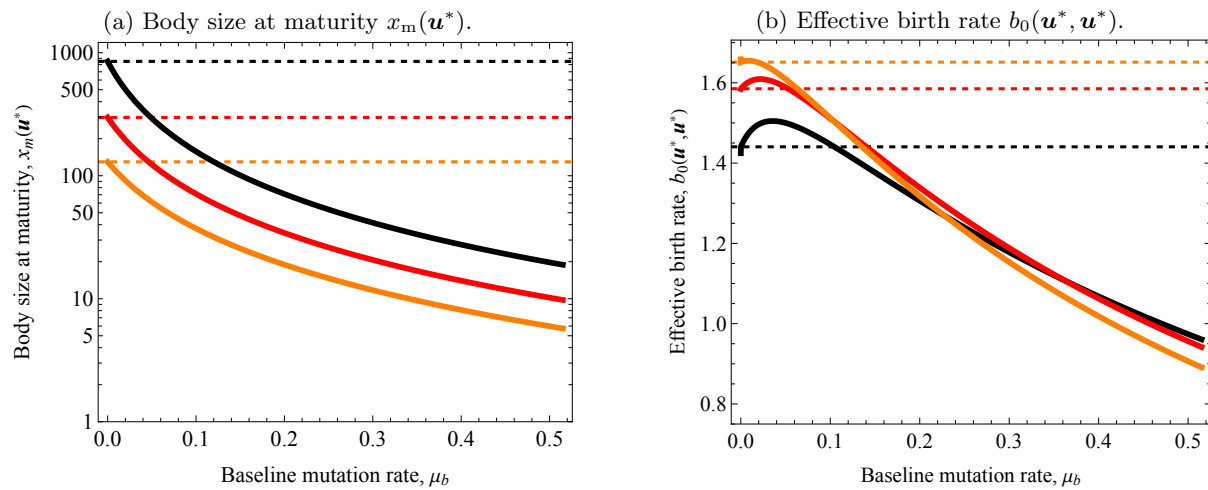


Figure 6: Predictions from the analytical model for the body size at maturity $x_m(\mathbf{u}^*)$ and the effective birth rate $b_0(\mathbf{u}^*, \mathbf{u}^*)$ at the uninhabitable population state as a function of baseline mutation rate for different values of mortality rate d_b ($d_b = 0.1250$ - black, $d_b = 0.1625$ - red, $d_b = 0.2$ - black). The dashed lines represent the “classical life-history” prediction (i.e. when $\mu(u_g^*) \rightarrow 0$ and $u_g^* \rightarrow 0$), where the colours of the dashed represent the different values for d_b parameter and match the values of solid lines ($d_b = 0.1250$ - black, $d_b = 0.1625$ - red, $d_b = 0.2$ - black). Parameter values: $\sigma = \sigma_b = \sigma_d = 0.2$, $x_0 = 1$, $a = 0.9$, $c = 0.75$, $\gamma = 0.00035$, $\beta = 1$, $\mu_f = 0$.